ELSEVIER

Quaternary Science Reviews 26 (2007) 3249–3275

QSR

Holocene relative sea-level change, isostatic subsidence and the radial viscosity structure of the mantle of northwest Europe (Belgium, the Netherlands, Germany, southern North Sea)

Annemiek Vink[a,*], Holger Steffen[b,1], Lutz Reinhardt[a], Georg Kaufmann[b]

[a]*Federal Institute for Geosciences and Natural Resources, Stilleweg 2, 30655 Hannover, Germany*
[b]*Institute of Geological Sciences, FU Berlin, Malteserstr. 74-100, Haus D, 12249 Berlin, Germany*

Received 5 July 2006; received in revised form 4 April 2007; accepted 23 July 2007

Abstract

A comprehensive observational database of Holocene relative sea-level (RSL) index points from northwest Europe (Belgium, the Netherlands, northwest Germany, southern North Sea) has been compiled in order to compare and reassess the data collected from the different countries/regions and by different workers on a common time–depth scale. RSL rise varies in magnitude and form between these regions, revealing a complex pattern of differential crustal movement which cannot be solely attributed to tectonic activity. It clearly contains a non-linear, glacio- and/or hydro-isostatic subsidence component, which is only small on the Belgian coastal plain but increases significantly to a value of ca 7.5 m relative to Belgium since 8 cal. ka BP along the northwest German coast. The subsidence is at least in part related to the Post-Glacial collapse of the so-called peripheral forebulge which developed around the Fennoscandian centre of ice loading during the Last Glacial Maximum. The RSL data have been compared to geodynamic Earth models in order to infer the radial viscosity structure of the Earth's mantle underneath NW Europe (lithosphere thickness, upper- and lower-mantle viscosity), and conversely to predict RSL in regions where we have only few observational data (e.g. in the southern North Sea). A very broad range of Earth parameters fit the Belgian RSL data, suggesting that glacial isostatic adjustment (GIA) only had a minor effect on Belgian crustal dynamics during and after the Last Ice Age. In contrast, a narrow range of Earth parameters define the southern North Sea region, reflecting the greater influence of GIA on these deeper/older samples. Modelled RSL data suggest that the zone of maximum forebulge subsidence runs in a relatively narrow, WNW–ESE trending band connecting the German federal state of Lower Saxony with the Dogger Bank area in the southern North Sea. Identification of the effects of local-scale factors such as past changes in tidal range or tectonic activity on the spatial and temporal variations of sea-level index points based on model-data comparisons is possible but is still complicated by the relatively large range of Earth model parameters fitting each RSL curve, emphasising the need for more high-quality observational data.

1. Introduction

The nature and magnitude of relative sea-level (RSL) movement (i.e. rise or fall or a sequence of events involving both) in any particular coastal or estuarine area since the Last Glacial Maximum (LGM) is determined mainly by three regional-scale factors which interact with each other: (i) the climatically induced global/eustatic increase in ocean water volume, (ii) tectonic subsidence or uplift of the crust and (iii) the glacio- and/or hydro-isostatic adjustment of the lithosphere in reaction to the mass redistribution associated with spatially and temporally changing ice, water and sediment volumes (e.g. Lambeck, 1997; Shennan et al., 2000a; Shennan and Horton, 2002; Milne et al., 2005). In northwest Europe, the post-glacial isostatic component is related mainly to the rebound of Fennoscandia and/or water and sediment loading of the North Sea Basin. Eustatic sea-level rise is a function of time only, whereas tectonic and isostatic subsidence/uplift are

*Corresponding author. Tel.: +49 511 6432392; fax: +49 511 6433663.
E-mail address: Annemiek.Vink@bgr.de (A. Vink).
[1]Institute of Geodesy, University of Hannover, Schneiderberg 50, 30169 Hannover, Germany.

0277-3791/$ - see front matter © 2007 Elsevier Ltd. All rights reserved.
doi:10.1016/j.quascirev.2007.07.014

functions of both time and position. Local-scale processes such as past modifications in tidal range, changing relationships between the local water table and sea level and/or changes in sample elevation due to sediment consolidation can additionally influence the registration of RSL changes in the sedimentary record (we refer to Van de Plassche, 1982; Shennan et al., 2000a, for a detailed account of these processes).

Numerous studies of Holocene RSL change in northwest Europe have been carried out in the past few decades which demonstrate that variations in RSL magnitude and trend do occur on both local and regional scales (e.g. Jelgersma, 1961; Louwe Kooijmans, 1974; Roeleveld, 1974; Ludwig et al., 1979; Linke, 1982; Van de Plassche, 1982; Shennan, 1987; Roep and Beets, 1988; Roeleveld and Gotjé, 1993; Denys and Baeteman, 1995; Kiden, 1995; Behre, 2003, 2007; Bungenstock, 2005). Although many regional RSL comparisons have been attempted (e.g. Lambeck, 1993a,b; Denys and Baeteman, 1995; Van de Plassche, 1995; Lambeck, 1997; Lambeck et al., 1998a; Beets and Van der Spek, 2000; Shennan et al., 2000a; Kiden et al., 2002; Shennan and Horton, 2002; Van de Plassche et al., 2005), discussion still continues as to the relative contribution and magnitude of glacio- and hydro-isostasy on differential RSL in these regions. For example, it has often been suggested that the sea-level changes which are recorded in supposedly tectonically stable and formerly ice-free areas such as northwest Europe should mainly reflect global ocean volume and climate change (e.g. Behre, 2003, 2007, for the German Bight). However, such a view conflicts strongly with the results of more geophysically oriented papers which show that the whole of northwest Europe up to southern France and even far-field sites such as the Caribbean may have been influenced by Post-Glacial isostatic movements associated with the melting of the Fennoscandian, British and Laurentide ice sheets (e.g. Lambeck, 1997; Lambeck et al., 1998a; Kiden et al., 2002; Milne et al., 2005).

Isostatic relaxation of the Earth's surface in response to the melting of the ice sheets occurs at a rate that is governed by the mechanical properties of the Earth, in particular mantle viscosity and lithosphere thickness. Thus, regional and even local differences in RSL can be used as input in order to model sea-level change using a variety of Earth and ice parameters (i.e. incorporating ice sheet reconstructions, Earth rheology and glacio- and hydro-isostasy). Results of comparative data analysis and geophysical modelling of Holocene glacio- and hydro-isostatic crustal movements in the Dutch North Sea sector and in the Belgian–Dutch coastal plain (Kiden et al., 2002) show that post-glacial isostatic lowering of the crust has definitely occurred in this area and that it increases significantly from the southwest to the northeast, although only eight North Sea index points were used in the analysis. Indeed, the area is close enough to the Fennoscandian ice sheet that it may be differentially affected by it, whereas the glacio-isostatic effects from other ice sheets such as the Laurentide or British ice sheets can be assumed to be near to negligible in the Belgian-Dutch area due to the larger distances and/or smaller volumes of ice involved. Kiden et al. (2002) attribute the isostatic subsidence of the crust to the last phase of the collapse of a peripheral glacial forebulge around the Fennoscandian ice sheet, which was previously reconstructed from both model and observational data and is assumed to have been centred in the North Sea between Norway and Great Britain, extending through northwest Netherlands and northern Germany (e.g. Mörner, 1980; Shennan, 1987; Fjeldskaar, 1994; Lambeck, 1995), and to hydro-isostatic subsidence of the North Sea Basin caused by water loading as sea level rose. Unfortunately, the establishment of more detailed patterns of crustal movement within this forebulge subsidence zone, including limits of maximum subsidence, has up to now been impossible due to the general scarcity of reliable older and deeper sea-level data (>8 cal. ka BP) from the southern North Sea region, which is the area and time in which differential isostatic movements are assumed to have been greatest.

Both Kiden et al. (2002) and Van de Plassche et al. (2005) state that new suites of data, preferably older than 8 cal. ka BP, should be collected in the northern part of the Netherlands in order to test model predictions of stronger isostatic subsidence there. In this paper, we attempt to do so without utilising more northern Netherlands data but rather by extending the data set to include many more samples from the northwest German sector (Behre, 2003, 2007) and the southern North Sea (compilation of published and new data, see Section 2.2.4). Until recently, German and several North Sea sea-level observational data were relatively inaccessible as they were chiefly published in local German journals. However, the extremely detailed synthesis of reliable German sea-level index points as published in German by Behre (2003) and later in English by Behre (2007) has opened the door for comparisons with sea-level data from neighbouring countries such as Belgium and the Netherlands. Thus, the first aim of this paper was to (i) critically reassess and compare valid sea-level index points from Belgium (Denys and Baeteman, 1995), Zeeland (Kiden, 1995), the western and northern Netherlands (Van de Plassche, 1982), the central Netherlands (Van de Plassche et al., 2005), northwest Germany (Behre, 2003) and the southern North Sea on a common time–depth scale so that RSL rise in northwest Europe can be directly compared and interpreted, and (ii) approximate the dimensions and rates of isostatic subsidence between the analysed regions following the methods of but expanding upon Kiden et al. (2002).

Definitive models for isostatic subsidence and the viscosity of the mantle beneath northwest Germany and the southern North Sea do not yet exist, although such data are essential for improving the resolution of Earth structure modelling in general. Thus, the second aim of this paper was to use geophysical models and the suite of available observational RSL data in order to infer the

radial viscosity structure of the Earth (lithosphere thickness, upper-mantle viscosity, lower-mantle viscosity) beneath Belgium, the Netherlands, northwest Germany and the southern North Sea; and conversely to use the resulting best-fit Earth models to predict RSL at any arbitrary location within the region specified by that model. Such predicted RSL curves have the potential to better constrain the possible structure and limit of maximum forebulge subsidence in northwest Europe.

Finally, our third aim was to compare predicted (model) RSL values with actual sea-level observations in order to identify possible effects of local-scale factors such as past changes in tidal range or tectonic activity on the spatial and temporal altitude variations of sea-level index points. Identifying local-scale factors is important in order to fine-tune index point RSL values and thus to improve the quality of both the observational RSL data themselves and the geophysical models which are dependent on them.

2. Data acquisition

2.1. Evaluation and standardisation of available sea-level observational data

2.1.1. Available data

The database of sea-level observational data derived from Belgium, the Netherlands, northwest Germany and the southern North Sea which has been used for this study is summarised in Appendix A and includes 133 basal peat dates, 13 dates from intercalated peat beds, 11 tidal-flat/salt marsh dates (e.g. in situ molluscs; contact between fresh and brackish muds), 14 dates based on organic remains in beach banks, tidal levees or on clastic Holocene (e.g. soils; roots/wood) and 67 archaeological/historical dates (e.g. past habitation levels; polder surfaces).

2.1.2. Indicative meaning of the sea-level data in terms of past tidal levels

Basal peats are especially important for the determination of former local water levels and form the backbone of all sea-level curves discussed in this paper. They were formed during the Late Pleistocene and Early Holocene, when the glacially exposed, gently inclined sandy palaeosurface of northwest Europe was gradually submerged by the transgressive North Sea. The sea-level rise raised the regional groundwater level, thus inhibiting drainage and initiating the development of telmatic (subaerial) basal peat in a narrow belt in front of the tidal area. However, the growth of this peat (''basis peat'' following Lange and Menke, 1967) did not last very long: the rising sea level quickly drowned the peat and a lagoonal or tidal-flat environment with clayey deposition followed.

In tidally influenced areas, telmatic basal peat growth begins at or slightly above the local mean high water (MHW) level. It is generally assumed that such a basal peat layer may approximately reflect coastal MHW in a relatively flat, open coastal area, but that it will rather reflect a different, local MHW level when, for example, coastal sand dunes, barrier systems or river outlets cause an extinction (lower MHW) or amplification (higher MHW) of the tidal wave (e.g. Jelgersma, 1961; Roeleveld, 1974; Van de Plassche, 1982, 1986). Tidal extinction or amplification of a tidal wave is largely controlled by (i) the floodbasin effect (e.g. Zonneveld, 1960; Van de Plassche, 1982, 1995), which causes a decrease in tidal amplitude (and hence of local MHW) in an upstream direction in an estuary or tidal channel due to the frictional dissipation of tidal energy in large intertidal storage basins; (ii) the estuary effect (e.g. Fairbridge, 1961), which causes an increase in tidal amplitude due to confinement of the tidal wave in a funnel-shaped embayment and/or (iii) the river gradient effect (e.g. Louwe Kooijmans, 1974; Cohen, 2005), which refers to a gently sloping groundwater surface in river areas and leads to a relative increase in local MHW altitude in a longitudinal upstream direction along the estuary. Depending on the amount of tidal extinction/amplification, basal peats thus tend to form at a local MHW level which can vary in depth between mean sea level (MSL) and coastal MHW or even above, but is never lower than MSL. This means that, strictly speaking, the position of the base of a basal peat resting on consolidated, non-marine Pleistocene sand can only be used to constrain an upper limit of MSL in a tidally influenced area (i.e. any altitude above MSL). Some basal peats may even have formed well above contemporaneous sea level under the influence of raised groundwater levels, e.g. in sheltered sand dunes due to convex water tables, and are thus sea-level independent. In contrast, the top of a basal peat has the potential to define the marine flooding contact and thus the lowest limit of the highest local MHW spring tide (local MHW–MHWS), provided that continuous sedimentation to the following lagoonal/brackish water clays can be assured and/or the presence of an erosional contact can be completely dismissed (e.g. through diatom analysis). Despite their clear difference in indicative meaning, both approaches allow no more than the reconstruction of local water-level conditions at the sample site, and their exact relationship to MSL or coastal MHW can only be indirectly deduced given and taken a number of assumptions (see Section 3.1). For a more detailed description of the complex relationships between basal peat formation and local water levels, we refer to Van de Plassche (1982, 1986).

In some areas (e.g. along the coast of NW Germany between the Ems and Elbe Rivers), peat layers are found which are intercalated between brackish tidal/lagoonal clayey sediments (e.g. Streif, 2004), the base indicating a regressive overlap to subaerial conditions (local MHW) and the top, if not erosive, a transgressive overlap (local MHW–MHWS). Although these peats can also provide information on former local sea levels and, more impor-

tantly, on RSL stagnancy phases, considerable care must be taken in using them as sea-level indicators as the compaction effects of both the peat and the underlying clay may have been considerable. Other sea-level indicators which have been used in this study include contact levels between fresh and brackish muds (~ local MHW), positions of in situ molluscs (depths slightly below local MHW, depending on the species) and organic remains in beach banks, tidal levees or dune soils (local MHW–MHWS). In the German data subset, habitation levels and fossil polder surfaces are used which are considered not to have formed far below local MHWS. For more detailed information on the exact indicative meaning of these sea-level data, we refer to the original articles from which they are derived (see Appendix A).

2.1.3. Altitude corrections

All sample depths were converted to the German Normalnull (NN) ordnance datum in order to allow direct comparison between the analysed regions. NN is an approximate value for MSL. The Dutch Nieuw Amsterdams Peil (NAP) ordnance datum is equivalent to NN as both systems are based on the same vertical bench mark datum in Amsterdam; the Belgian Tweede Algemene Waterpassing (TAW), however, lies 2.33 m below NAP/NN and sample depths were thus adjusted accordingly. Altitude accuracy of samples derived from land boreholes or open pits/outcrops was, save several exceptions, generally good at ca ± 0.10 m, this value being comprised mainly of errors associated with levelling and sampling. For the North Sea samples, altitude accuracy greatly decreased due to the still problematic instrumental determination of exact water depth from the ship, possible compression or extension of core material during the vibrocoring process and the conversion of time-/tidal-dependent water depth to depth below NN, which is based on comparison with tide gauge measurements which often lie far away from the sample positions. For these samples, an accuracy of not less than ± 1.0 m had to be assumed.

The compaction of peat and/or of silty and clayey layers underlying the peat or a particular habitation level is a problem which under certain circumstances can greatly alter the depth of a sea-level index point. Whether compaction occurs depends on several factors, including initial water content of the material, lithology, particle size and shape, age and the thickness and nature of the overburden. As these factors vary in their dimensions from sample to sample even within a small local area, samples possibly influenced by compaction (35 samples in our data set) have not been depth corrected. However, a rough estimate of compaction, calculated by simply assuming 50% compaction of the original peat beds (i.e. a compaction factor of 2 following Van de Plassche et al., 2005), is provided in Appendix A. Samples in which compaction effects were assumed by the original authors or by the estimation provided above to be >0.6 m, were not considered in this study.

2.1.4. Age conversions

All original ^{14}C dates were calibrated to calendar years BP using the CALIB 4.4 conversion routine (Stuiver and Reimer, 1993; Stuiver et al., 1998; http://calib.qub.ac.uk/calib/). The 1σ confidence interval (68%) in the calendar age ranges was used in the construction of sea-level curves. Pre-1962 radiocarbon dates from Groningen, as derived from Bennema (1954) and Jelgersma (1961) and used in the Zeeland and western Netherlands curves, have not been corrected for isotopic fractionation effects (δ^{13}C correction). In the publication of Van de Plassche (1982), a correction of -40 radiocarbon years has been used, based on the assumed average composition of freshwater peat. However, as highlighted by Kiden (1995), isotopic fractionation effects not only depend on the nature of the dated material but also on laboratory procedures, and so a correction was not carried out in this analysis but was considered as a possible extension of the age range of the samples under consideration in the respective sea-level curves (Figs. 2 and 3).

2.2. The database

A list of the 238 index points used in this paper, together with all the relevant information concerning these samples, is provided in Appendix A. Only those samples which were considered as valid sea-level index points by the original authors were selected; geographic positions are shown in Fig. 1. For better comparison and clarity, sample numbers/codes in Appendix A and in the individual sea-level curves (Figs. 2–4) always refer to those provided by the original authors.

2.2.1. Belgium

Basal peat data derived from the Belgian coastal plain have been reassessed in terms of local tide water levels in Denys and Baeteman (1995) and were used as the basis for the Belgian data set in this paper. Many of the samples in the data set of Denys and Baeteman (1995) were found to be unreliable by those authors, and so only the 21 most reliable samples remaining after their critical data analysis, covering the time span from 9.5 to 3 cal. ka BP, were selected here (Appendix A; Fig. 2A). Both bases and tops of peat layers were used; tops were taken only when no visible signs of erosion were found (e.g. through diatom analysis). The area under consideration is crossed by only one small river, the IJzer, and edaphic dryness during the Early Holocene explains why the effects of local seepage and river gradient effects on the altitude of peat formation were found to be limited or even absent on the Belgian coastal plain. However, several samples derived from the tops of thicker peat layers (0.2–0.4 m) may have experienced some compaction. Error envelopes for local MHW and for the upper limit of MSL were drawn, depending on the indicative meaning of the dated peat layers as determined by the original authors (Fig. 2A).

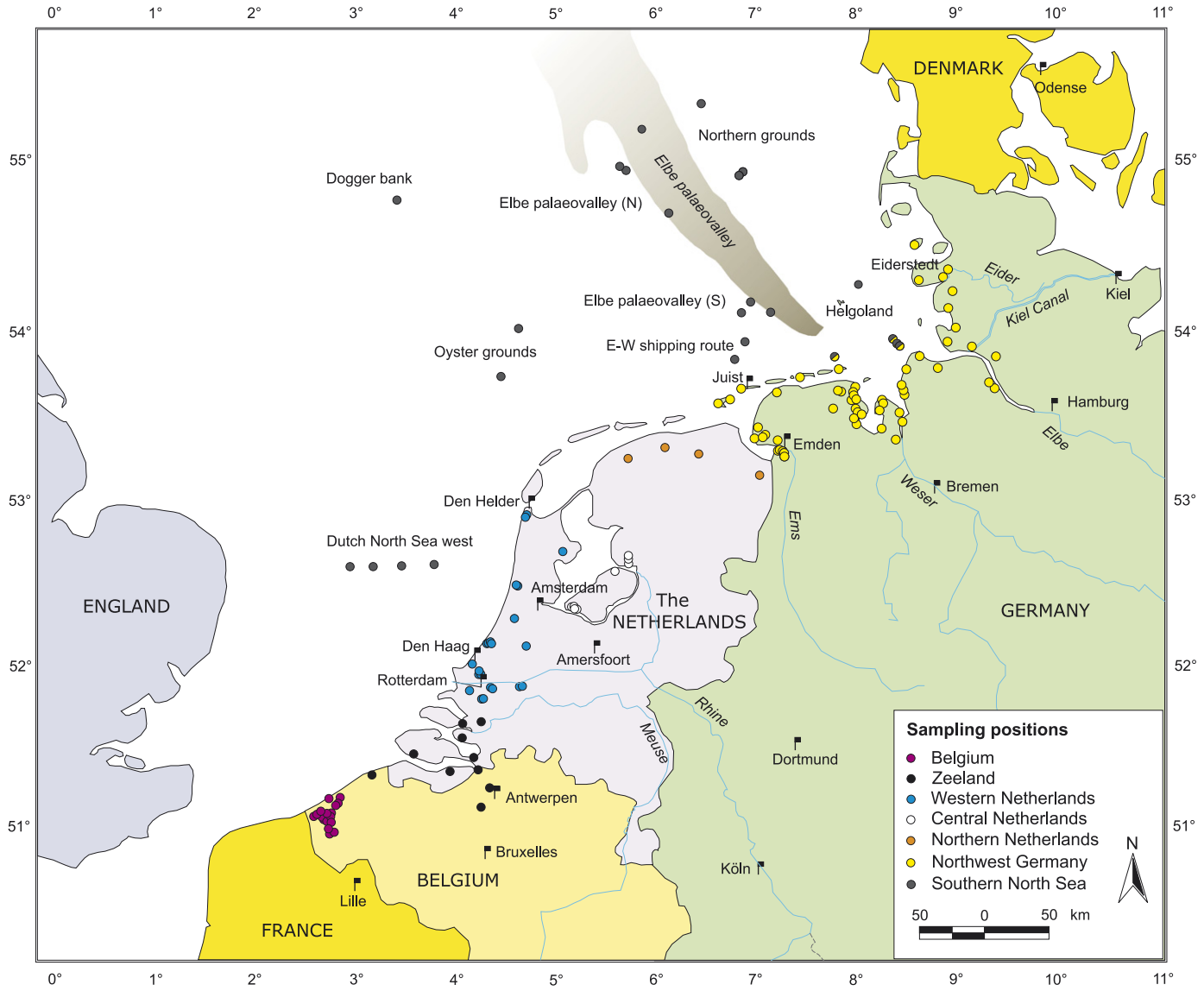

Fig. 1. Locations of index points used for the determination of Holocene RSL rise in Belgium, the Netherlands, northwest Germany and the southern North Sea. More than one index point can be derived from each sample site where several samples were taken from the same core/outcrop or where samples lie very close to each other.

2.2.2. *The Netherlands*

2.2.2.1. Zeeland. Sea-level index points (mostly bases of basal peats) derived from Zeeland and the adjacent estuarine flood plain of the River Schelde in northern Belgium have been obtained from Kiden (1995) and the publications cited therein, and were used to produce an error envelope for the upper limit of MSL for Zeeland covering the time period of approximately 8–4 cal. ka BP (Fig. 2B). As the peat samples were generally thin (2–5 cm) and came from the bases of the basal peats which rest directly on the sandy Pleistocene subsoil, compaction effects were considered to be negligible. However, Kiden (1995) found that a large number of his Zeeland index points exhibited relatively high but variable positions in comparison to the western Netherlands MSL envelope, and attributed this to the interaction between the pronounced local Pleistocene morphology and topography, differential palaeo-groundwater levels and the variable influence of floodbasin and river gradient effects on the altitude of peat growth. Nevertheless, samples derived directly from the Schelde palaeovalley (e.g. samples 4, 10, 11, 27) exhibited a relatively low time–depth position and appeared to have been influenced far less by local and regional groundwater effects (Kiden, 1995). He thus concluded that although a large number of the Zeeland sea-level index points had to be considered unreliable, the lowermost points could still provide a good estimation of MSL in the area. Twelve of these more reliable points have been included in this study (Appendix A; Fig. 2B).

2.2.2.2. Western and northern Netherlands. A relative (upper limit of) MSL curve for the western and northern

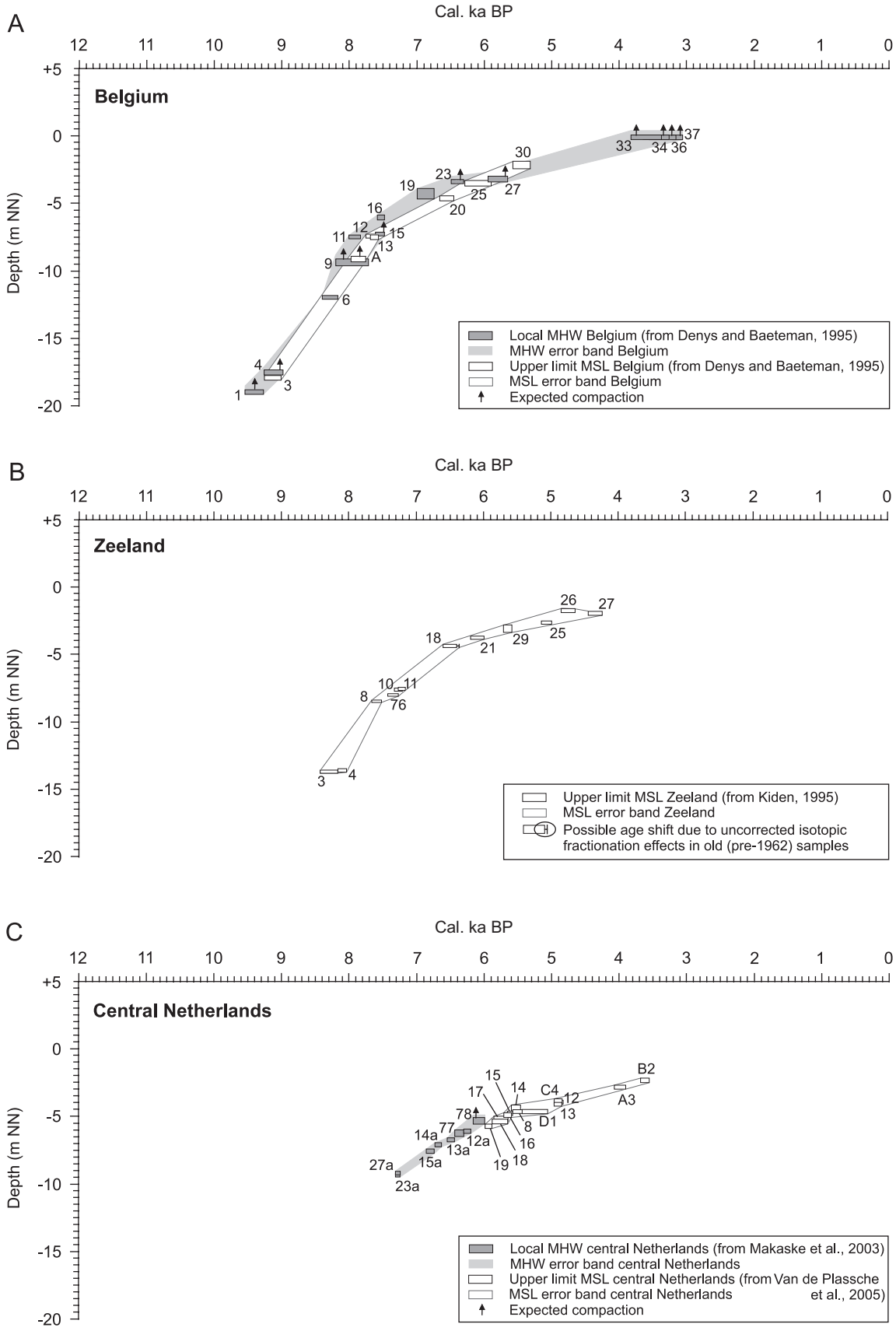

Fig. 2. Age–depth distribution of sea-level index points obtained mainly from basal peat data from (A) Belgium (after Denys and Baeteman, 1995), (B) Zeeland (after Kiden, 1995) and (C) the central Netherlands (after Makaske et al., 2003; Van de Plassche et al., 2005). The widths of the error boxes represent the 1σ-calibrated age range of the conventional radiocarbon age; the height corresponds to the total vertical error in sample altitude. Depending on the indicative meaning of the basal peats under consideration, error bands/envelopes have been drawn for local mean high water (MHW) and/or the upper limit of mean sea level (MSL). Samples in which some compaction may be expected are marked by an upward arrow.

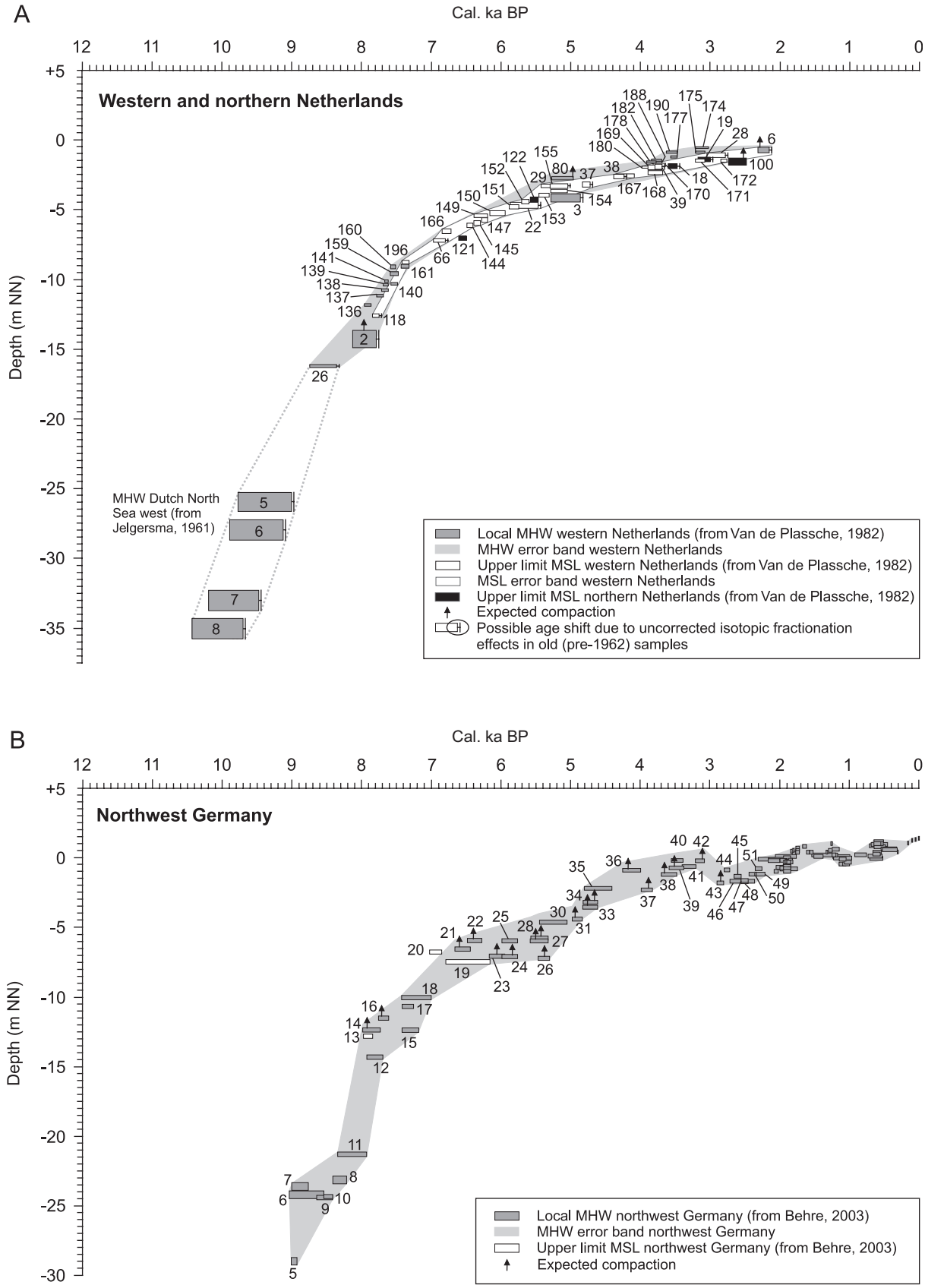

Fig. 3. Age–depth distribution of sea-level index points obtained from basal and intercalated peat data as well as archaeological data from (A) the western and northern Netherlands (after Van de Plassche, 1982); but including four North Sea index points from offshore western Netherlands (after Jelgersma, 1961) for a rough estimation of Early Holocene sea-level rise in this area, and (B) northwest Germany (after Behre, 2003). The widths of the error boxes represent the 1σ-calibrated age range of the conventional radiocarbon age; the height corresponds to the total vertical error in sample altitude. Depending on the indicative meaning of the index points under consideration, error bands/envelopes have been drawn for local mean high water (MHW) and/or the upper limit of mean sea level (MSL). Samples in which some compaction may be expected are marked by an upward arrow.

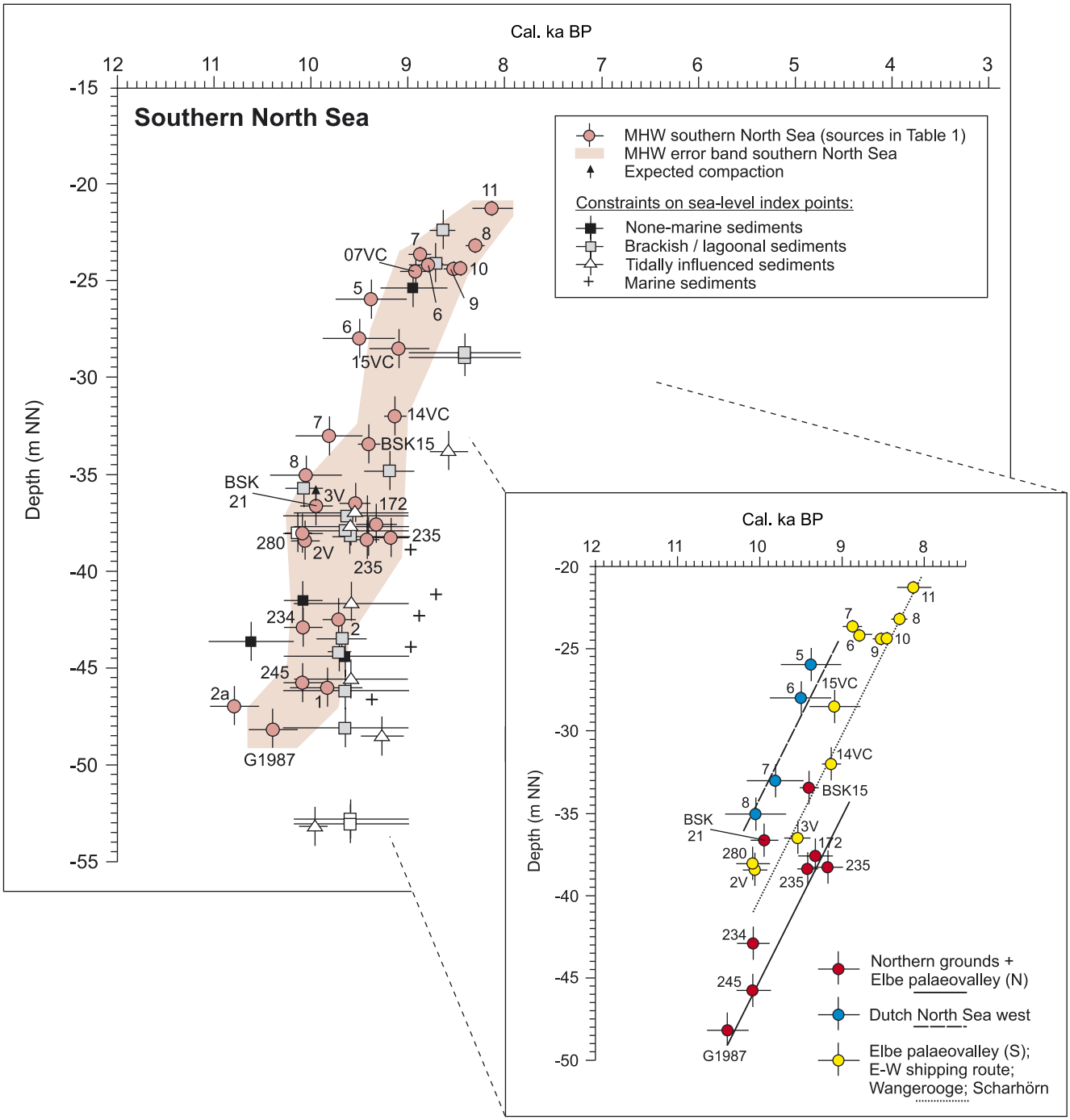

Fig. 4. Age–depth distribution and local mean high water (MHW) error band of sea-level index points obtained from basal peat data from the southern North Sea (data compiled from different sources; see Appendix A). Index points 6–11 of the northwest German data set have been included as they are derived from offshore, near-coastal areas (Wangerooge, Neuwerk, Scharhörn). The horizontal error bars represent the 1σ-calibrated age range of the conventional radiocarbon age; the vertical error bars correspond to the total vertical error in sample altitude. Samples in which some compaction may be expected are marked by an upward arrow. Constraints on the possible width of the error envelope are provided by dated non-marine, brackish, tidally influenced and fully marine sediments derived from Ludwig et al. (1979), Streif et al. (1983) and from unpublished new data of the BGR. Differences between RSL trends in three major sub-regions of the North Sea (inset) clearly reveal the effect of geographically controlled differential rates of Post-Glacial isostatic and/or tectonic subsidence.

Netherlands, derived mainly from basal peat data, was presented and its characteristics discussed in detail by Van de Plassche (1982, 1995). His curve encompasses the time interval from ca. 8–2 cal. ka BP and was obtained from a critical comparative analysis of old data with the inclusion of new data from the Rhine region and the coastal beach-plain area of the former Older Rhine Estuary to the north of Rotterdam. We have used the analyses of Van de Plassche (1982, 1995) as the basis for obtaining reliable index points for the western Netherlands, and our resulting

local MHW and upper limit of MSL curves are constrained by 42 sea-level index points from the Rhine–Meuse River dune and beach-plain area and six index points from the province of Noord-Holland (W–NW Netherlands) (Appendix A; Fig. 3A). In the light of growing evidence that differential Post-Glacial isostatic crustal adjustment and/or tectonic movement did occur in the Netherlands (Kiden et al., 2002; Kooi et al., 1998, respectively), we decided not to integrate the five index points from the northern Netherlands into the western Netherlands MSL error band, although their positions have been superimposed onto the western Netherlands curve for comparative reasons (Fig. 3A). Unfortunately, the number of reliable northern Netherlands sea-level index points is still too low to create a separate MSL curve for that region. The index points derived from aeolian sand dunes in the Rhine and Meuse River areas (mainly bases of basal peats) are especially difficult to interpret in terms of their indicative meaning in relation to rising sea level, as the chances of independent peat growth due to higher local (ground)water tables caused by the river gradient effect, seepage and/or hampered drainage are relatively high in this deltaic area (Van de Plassche, 1982). Furthermore, the floodbasin effect and a lack of evidence for marine influence means that most of these index points can only provide upper limit of MSL information. Compaction effects can, however, be precluded for most of these samples due to their position in the very base of the basal peats, directly on the dune sands. In contrast, samples from the beach-plain areas appear to be easier to quantify in terms of former local and even coastal MHW levels (e.g. Van de Plassche, 1995). Details of reliable as well as unreliable index points and all the problems involved in the stringent selection of data are provided by Van de Plassche (1982).

2.2.2.3. Central Netherlands. Roeleveld and Gotjé (1993) reconstructed the Mid-Holocene water-level rise in the area of Schokland (central Netherlands) using two suites of (near-)basal peat samples from the slopes of two aeolian sand dunes. The resulting MSL curve was found to consistently lie somewhat below that of the western Netherlands, leading to slight confusion and consequently to the retrieval of new data and a critical reassessment of the central Netherlands curve by Van de Plassche et al. (2005). Nineteen reliable basal peat sea-level index points resulting from that comparative analysis, and two from the original western Netherlands curve (Van de Plassche, 1982), were used to form the central Netherlands data set of this study (Appendix A). The data cover the time interval from 7.5 to 3.5 cal. ka BP and were used to produce error envelopes for local MHW and the upper limit of MSL for the area (Fig. 2C). Samples were taken near or from the base of peat layers and so compaction effects are considered to be negligible. Van de Plassche et al. (2005) did calculate a compaction factor of 2 for samples derived from slightly above the surface of the dune sand, but this leads to a compaction correction of 0.07 m at the most. The effects of local (ground)water gradients on the development of peat in the area have not been quantified, but may well have been small considering the generally low age–depth positions of the index points compared to the western Netherlands curve.

2.2.3. Northwest Germany

A detailed relative MHW curve for northwest Germany has recently been published by Behre (2003, 2007) based on the collection and synthesis of all reliable sea-level index points which had been collected from the coastal regions of the German Bight throughout the last few decades. The samples are derived from a relatively large geographical area (see Fig. 1), including the Ems, Weser, Elbe and Eider River mouths/estuaries and ranging from Emden in the southwest (East Frisia; Lower Saxony) to Eiderstedt in the northeast (Schleswig-Holstein). The curve is based on an extensive data set containing 110 sea-level index points, of which 45 cover the time interval from ca 9–2 cal. ka BP, the rest being younger (Appendix A; Fig. 3B). Most of these younger dates are derived from archaeological or historical data; the older dates are based mainly on the analysis of basal and intercalated peats or tidal-flat/salt marsh depositional systems. According to Behre (2003), levels representing storm tide heights (MHWS) such as old habitation surfaces, or heights located between local MHW and MHWS such as old polder surfaces, must have reached ca 0.4–1 m above local MHW along the German Bight, depending on the exact situation and geographical location. We refer to the work of Behre (2003) for a detailed account of individual index point altitude conversion to MHW for such archaeological samples. Most of the older samples in the data set already refer to local MHW level as they are derived from the transgressive tops of basal peats and/or from intercalated peats (see Appendix A). Intercalated peats are especially vulnerable to compaction of the peat as well as the underlying intermediary clay, and a depth reduction of about half a metre may be expected for a few index points of the data set (e.g. samples 33, 37, 42). Due to the compaction problem and the widespread geographical distribution of data points, the local MHW envelope for northwest Germany is relatively wide in comparison to those of Belgium and the Netherlands (Fig. 3B).

2.2.4. The southern North Sea

The basal peats which are required to improve our still very fragmentary knowledge of the Earliest Holocene transgressional history of the North Sea Basin (i.e. sea-level rise before ca 8 cal. ka BP) formed relatively far offshore from the present-day coastline and can thus only be obtained during time-consuming and costly ship cruises. Furthermore, the chances of encountering basal peats offshore are extremely small and the recovery method still follows a trial and error principle, because (i) the basal peats are generally extremely thin (often <5 cm) due to the rapid rate of RSL rise which did not encourage extensive

peat growth at that time, and so they do not show up diagnostically on seismic or echosound profiles, (ii) large tidal channels have probably eroded the basal peat and the underlying deposits in many places and (iii) the sampling process is greatly hampered by the fact that the overlying marine sands are generally very coarse, which at the moment means that fairly economical cores can only be taken using a vibrocorer which has a maximum penetration depth of 6 m. Nevertheless, several reliable index points have been obtained from the southern North Sea region during the last few decades, and these are summarised in Appendix A and Fig. 4. Four of these index points were used by Behre (2003) to constrain the older/lower part of his German MHW curve (sample sites 1, 2, 235, 172), of which the latter two are derived from the early work of Ludwig et al. (1979) in the North Sea Basin. In fact, Ludwig et al. (1979) and Streif et al. (1983) documented and palynologically dated several more basal peat layers derived from the western rim of the Elbe palaeovalley, and five of these have been included in this analysis (sites 234, 245, 280, H15/2V, H18/3V). The age–depth positions of the first three index points in this list were found to be slightly problematic as (i) their exact altitude could not be determined properly on board due to deficient measuring instruments, meaning that sample depth below NN could only be estimated afterwards using available bathymetric data of the area, and (ii) unambiguous palynological dating was not always possible due to large quantities of reworked components and/or bad preservation (Streif et al., 1983). They are nevertheless used here due to the present lack of better data from these areas and because their time–depth positions appear to be quite credible at the moment (Fig. 4). Six sites from the Dutch North Sea sector are originally derived from Jelgersma (1961) and Jelgersma et al. (1979) and are summarised in Kiden et al. (2002). Last but not the least, five new (bulk) basal peat data obtained by the German Federal Institute for Geosciences and Natural Resources (BGR) during North Sea cruises in 2004/2005 (Kudraß et al., 2004; Reinhardt et al., 2006) have been included.

In contrast to many of the peat layers derived from (river-influenced) dune/barrier systems or sheltered, coastal areas in which the exact relationship to MSL is often difficult to reconstruct, Early Holocene North Sea peats presumably developed under the direct influence of the rapidly rising sea level on the gently undulating Pleistocene substratum and thus likely approximate coastal rather than local MHW levels. Compaction effects can generally be ruled out as these thin peats lie directly on thick layers of sandy Pleistocene (Weichselian) sands. However, the available sea-level index points are derived from a geographically extensive area in which significant variations in isostatic and/or tectonic subsidence are expected, producing a broad MHW error band which can be up to 10 m wide (Fig. 4). This is in part caused by the large error bars involved in measuring sample altitude. Nevertheless, the comparison of age–depth values of index points derived from smaller selected areas of the North Sea clearly reveals a lower position of the northern Elbe palaeovalley + Northern grounds index points (see inset of Fig. 4) in comparison to those positioned closer to the northwest German coast, which in turn are positioned lower than those of the western Dutch North Sea. Despite these clear trends, intra-regional differences are observed which must be attributed to inadequate shipboard/bathymetrical depth measurements, age over- or underestimation due to reworking of older material or selective root rejuvenation of peat, respectively, or to sea-level independent peat growth in local landscape depressions. Nevertheless, deeper and older (North Sea) sea-level index data are extremely important for our understanding of early Post-Glacial ice sheet dynamics and the rates of initial sea-level rise, and they help to adjust and fine-tune geophysical models which aim at reconstructing past palaeogeographies and tidal ranges (e.g. Shennan et al., 2000b) as well as resolving the viscosity structure of the Earth's mantle (e.g. Lambeck et al., 1998a; Steffen and Kaufmann, 2005).

3. Methods of data analysis

3.1. Conversion of local sea-level data to MSL

Perhaps the greatest problem in comparing sea-level data from the different regions is that local MHW and MSL data cannot be directly compared with one another. Whereas local water levels can be more or less directly observed in the dated sea-level observation points, the water level at sea (MSL, coastal MHW) can only be indirectly deduced from these local data. Moreover, coastal MHW is a function of the tidal range of the studied area and varies greatly from region to region (e.g. present-day coastal tidal range decreases considerably in a north-easterly direction along the Belgian–Netherlands coast, being ca 3.8 m close to the Belgian border but only 2.3 m at the mouth of the River Meuse and 1.4 m in Den Helder). Despite these fundamental issues, a lower limit of MSL can be derived from the MHW data by subtracting the approximate present-day difference between MSL and coastal MHW (i.e. the tidal amplitude) at each sample location when we assume that (i) the effects of tidal extinction/amplification for "inland" samples have been near to negligible, and (ii) the tidal range at sea has remained near to constant over the time interval under consideration. The total vertical error range, calculated as the square root of the sum of squares of sample thickness, altitudinal error, indicative range and tide level error (e.g. Shennan et al., 2000a), increases significantly due to the inclusion of errors involved in defining the indicative meaning (taken as ±0.2 m) and the past tidal range (also ±0.2 m). In the case of upper limit of MSL data, index points represent any level between MSL and coastal MHW or even above, but are never lower than MSL. Thus, although detailed field knowledge and data analysis can eliminate a great deal of the uncertainty in the indicative

meaning, all we can conclude is that true MSL will have been lower than or equal to the altitude of such index points. Assuming that the index point formed between MSL and coastal MHW, a negative error in the indicative range arises which should approximately correspond to the tidal amplitude of that area. No positive error in indicative range exists as it is physically impossible that MSL was ever higher than the index point itself. Estimations of MSL and associated errors for all selected index points of this study are summarised in Appendix A.

MSL ranges (i.e. estimated MSL ± MSL error) are biased mainly by the underlying assumption that tidal ranges have not changed significantly during the last 10 ka, although there is no direct evidence that this is the case. In fact, palaeotidal models for the southern North Sea indicate lower tidal ranges during the Early Holocene (Franken, 1987; Austin, 1991; Shennan et al., 2000b) and only minor changes since ca 6 cal. ka BP, consistent with the changing palaeogeographies and coastline configurations at that time. Nevertheless, Roep and Beets (1988) did reconstruct a slightly higher tidal range along the western coast of the Netherlands before ca 5 cal. ka BP. Furthermore, neglecting the effects of tidal dampening can in many cases lead to an overcorrection of MHW data to MSL (especially in regions like Belgium and Zeeland where present-day tidal amplitudes are high). Consequently, MSL values derived from MHW data may be lowered too much with respect to the upper limit of MSL data, which only experience the overcorrection through their altitudinal error band. As such, we consider that the calculation of MSL using present-day coastal tidal ranges is not faultless or precise, but represents the most acceptable method for the direct comparison and modelling of sea-level data from different regions until more information on past coastal and local tidal ranges becomes available.

3.2. Determination of relative tectonic and isostatic subsidence

The difference in altitude between the MSL records of two regions reflects the total differential crustal movement between those regions and is generally composed of a local/regional tectonic component and an isostatic component. Only consistently small altitude differences (e.g. 200–300 yr) can be explained by non-geophysical processes such as aging effects caused by the presence of older carbon in the dated material (e.g. Van de Plassche et al., 2005). Long-term tectonic movements can be roughly estimated from the present-day depth of submerged Eemian sea-level highstand data (e.g. Kiden et al., 2002; Streif, 2004). Such estimations are based on the assumptions that (i) the Eemian highstand sediments in different regions are isochronous with an age of exactly 125 ka and were deposited on an originally more or less horizontal plane, and (ii) selected Eemian sea-level highstand data are representative of an entire region, thus neglecting the possibility of local-scale (neo)tectonics and non-linear tectonic movement (at a scale of tens of kilometres) during the studied time interval. These assumptions do not always hold (e.g. Schellmann and Radtke, 2004). The error introduced by assumption (i) is relatively small over the timescale under consideration (e.g. an age difference of 3 ka produces an error of $<2.5\%$). However, Kooi et al. (1998) have shown for the Netherlands that complex differential, short-term ($\sim$100 yr) crustal subsidence occurs in addition to long-term tectonic movement. Thus, sediments may well have experienced spatially variable and increased subsidence rates in (sub)recent times, and so we have double checked the values obtained from Eemian data with mean tectonic rates obtained by backstripping of Cenozoic stratigraphy at the timescale of the entire Quaternary (Kooi et al., 1998). The present lack of dated Eemian highstand sediments from the southern North Sea region means that we can only use the isopach map of the total thickness of Quaternary sediments in the North Sea (Caston, 1979) and the sedimentation rates determined from it as an approximate measure of long-term tectonic subsidence in these regions. In a broad sense, we consider this approach to be acceptable as the pattern of relative uplift or subsidence of currently known Eemian highstand sediments from the whole North Sea region (i.e. from England and Denmark to the coastal zone of the Netherlands) does fit well with this isopach map (Streif, 2004).

Following Kiden et al. (2002), subtraction of the (maximum) tectonic component/tectonic difference between two regions from the total differential crustal movement can be used as an approximate measure of the (minimum) isostatic component between those regions. We have used this method to analyse the influence of isostatic subsidence on northwest Germany, the western Netherlands and several southern North Sea sites in relation to Belgium.

3.3. Geodynamic modelling

The standardised data set of RSL in NW Europe as summarised in Appendix A can be used for geodynamic modelling of the Earth's internal structure. As glacial isostatic adjustment (GIA) is mainly controlled by the viscosity of the Earth's mantle and the thickness of the lithosphere, it is possible to investigate and determine the regional radial structure of the Earth with the help of an Earth model, a global ice and ocean model and the observational data mentioned above. The applied models and the calculation method have been extensively described in Steffen and Kaufmann (2005). Hence, the methodology is summarised only briefly here and we refer to the above-mentioned article for more detailed information.

3.3.1. Earth model

Model predictions are carried out using a spherically symmetric, compressible, Maxwell-viscoelastic Earth model. The elastic structures of the adopted Earth models are based on the seismic preliminary reference earth model

(PREM; Dziewonski and Anderson, 1981), and lithosphere thickness is taken as a free parameter. Mantle viscosity is parameterised into several sub-lithospheric layers with constant viscosity within each layer. The lower boundary condition is the Earth's core, which is assumed to be inviscid. In this paper, two sub-lithospheric viscosity layers have been assigned to an upper- and lower- mantle layer with constant viscosity, respectively. Thus, together with the free parameter lithosphere thickness, sea-level predictions are calculated for a three-layer Earth model. Recently, modelling investigations for GIA have changed from 1D and 2D inversion methods (e.g. Lambeck, 1993a,b; Lambeck et al., 1996, 1998a,b) to 3D flat (e.g. Kaufmann and Wu, 1998a,b; Wu et al., 1998; Kaufmann et al., 2000; Kaufmann and Wu, 2002; Kaufmann et al., 2005; Wu, 2005; Steffen et al., 2006) and spherical finite element models (e.g. Wu, 2002; Wu and Van der Wal, 2003; Zhong et al., 2003; Latychev et al., 2005a,b; Wu et al., 2005; Spada et al., 2006). However, we have chosen the 1D inversion method here as it is simple, efficient and, in comparison to former 1D investigations, the small distance between the different regional data sets might provide more precise information concerning the Earth's 3D structure in NW Europe. The search range of possible parameter values has been set between 60 and 160 km for lithospheric thickness H_l, between 10^{19} and 4×10^{21} Pa s for the upper-mantle viscosity η_{UM}, and between 10^{21} and 10^{23} Pa s for the lower-mantle viscosity η_{LM}.

Surface deformation is calculated by loading each Earth model with predetermined ice loads. Using the sea-level equation of Farrell and Clark (1976) for a rotating Earth, which can be rewritten as an integral equation which we solve iteratively, we can then derive RSL change (ΔRSL). ΔRSL is compared to the observational data and the best-fit Earth model is chosen.

3.3.2. Ice and ocean model

For the Late Pleistocene glacial ice-load history, the global ice model RSES (Research School of Earth Sciences, Canberra) is used. RSES incorporates Late Pleistocene ice sheets over North America, northern Europe, Greenland, the British Isles and Antarctica. The reconstructions are based on glaciological and geomorphological evidence and thus reflect the approximate extent of the Late Pleistocene ice sheets throughout the Last Glacial cycle. The model has been converted from the radiocarbon timescale to the sidereal timescale using the CALIB 4 conversion program (Stuiver and Reimer, 1993; Stuiver et al., 1998). The ice volume at the LGM, approximately 21.4 cal. ka BP, corresponds to 124 m of eustatic sea-level change. The vanishing ice volume is added time dependently to the ocean volume, thus affecting the hydro-isostatic component.

The ice extent for four different epochs, starting at the LGM, is shown in Fig. 5. It reflects the retreat of the large Weichselian ice sheet from a multi-dome complex covering Scandinavia and the Barents Sea to land-based ice sheets over Svalbard, Franz-Joseph-Land and Scandinavia. According to the model, the ice sheet disappeared around 9 ka ago.

3.3.3. Observational data

The sea-level observational data from NW Europe as presented in Appendix A have been grouped into three main regional subsets for geophysical modelling calculations (Belgium, the Netherlands and Germany), in such a way that each subset comprises data points which lie within a characteristic part of the "banana" shape of the Fennoscandian forebulge as shown in Fig. 2 of Kiden et al., 2002. Additional data sets, including (i) all locations, and (ii) only offshore data, were tested as well. Several of the index points in Appendix A have been used in more than one data set, depending on their locality. Thus, five data sets were arranged as follows (total number of index points in brackets):

- Belgium (33), consisting of 21 Belgian and 12 Zeeland sea-level index points.
- The Netherlands (76), encompassing the remaining 69 Netherlands index points after excluding five points from the northern Netherlands (these have been added to the German data set), six Dutch North Sea points and one point from the Dogger Bank.
- Northwest Germany (129), comprising the northwest German data set with 110 index points, five points from the northern Netherlands and 14 German North Sea index points.
- Southern North Sea (27), including 21 North Sea locations and six German coast index points (index points 6–11).
- Northwest European coast (238), a data set of all index points.

As compaction may have altered the altitude of some MSL data by up to 0.6 m (Appendix A) and has potentially influenced our model predictions (especially in the northwest German data set where several of the index points are derived from intercalated peats), an additional "test" data set was produced in which the MSL values were tentatively corrected for compaction by simply assuming 50% compaction of original peat beds (Appendix A). Compaction corrections were carried out for 11 index points from the Belgian data set (33% of the total data points), two index points from the Netherlands (3%), 20 points from northwest Germany (16%), one point from the southern North Sea (4%) and thus for a total of 33 index points from the entire northwest European coast data set (14%). Although it would be extremely interesting and more precise to correct sample altitude for tectonic activity, a factor which is actually not taken into account in the isostatic rebound models, the lack of suitably young and reliable (local) tectonic subsidence rates at our sample sites does not allow such a correction at this stage.

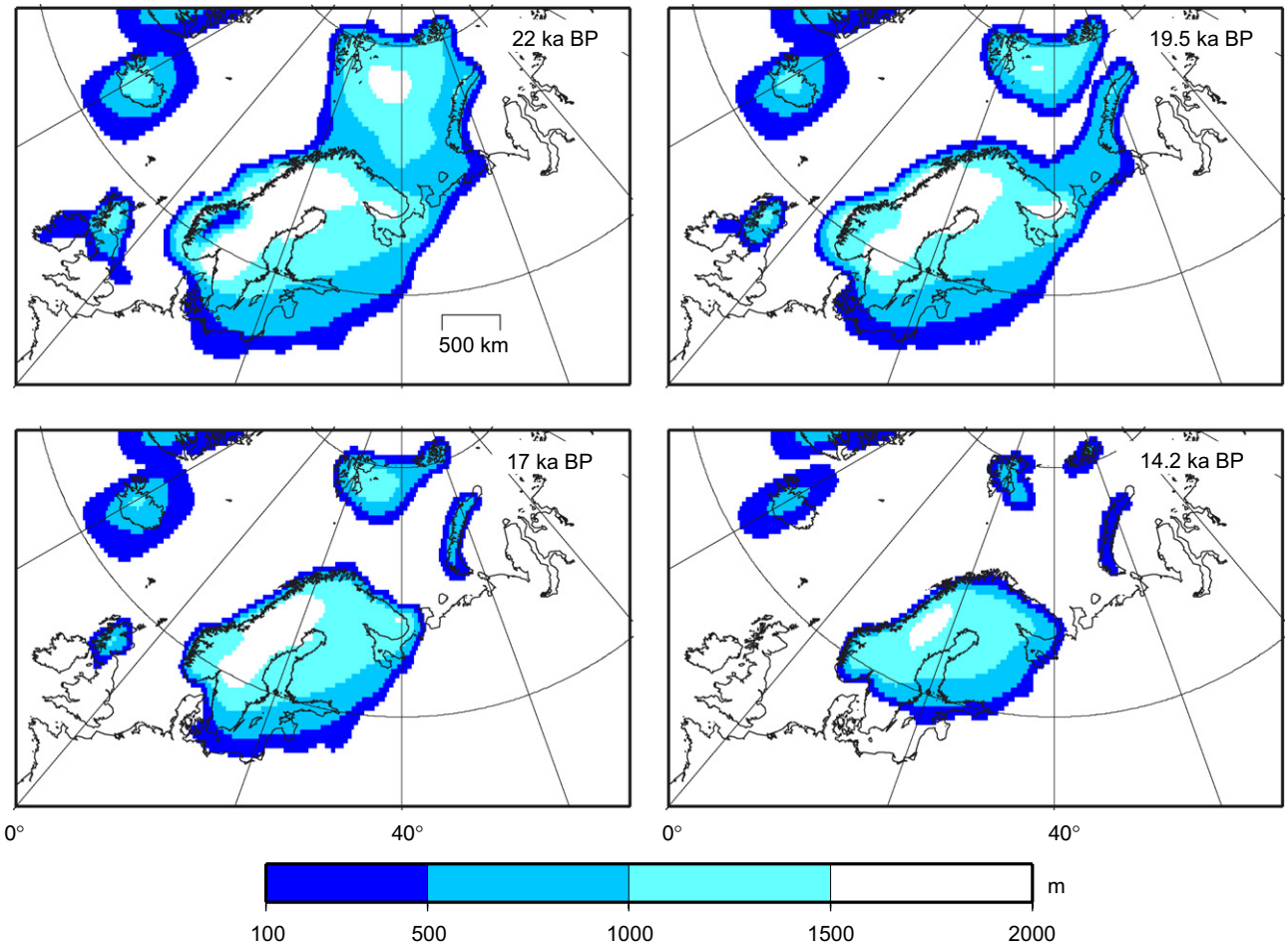

Fig. 5. Map of ice model RSES over Europe for four different time epochs. Contours represent 500 m height intervals.

3.3.4. Determination of the best-fit Earth model

A range of predicted RSL changes are compared to the subsets of sea-level observational data in order to determine best-fit Earth models for the different regions under consideration. This comparison is based on a least-squares misfit, defined as

$$\chi = \sqrt{\frac{1}{n}\sum_{i=1}^{n}\left(\frac{o_i - p_i(a_j)}{\Delta o_i}\right)^2}, \quad (1)$$

where n represents the number of observations considered, o_i the observational RSL data, $p_i(a_j)$ the predicted RSL for a specific Earth model a_j and Δo_i the data uncertainty. The search for a minimum value of χ within the parameter space produces an Earth model a_b, which fits the observational data set best. In the ideal situation that the model is complete and the observational uncertainties are normally distributed with known standard deviations and uncorrelated, the expected best fit would be $\chi = 1$. To bracket all Earth models that fit the observational data equally well as the best-fit Earth model a_b within the observational uncertainties, a confidence parameter is calculated as follows:

$$\Psi = \sqrt{\frac{1}{n}\sum_{i=1}^{n}\left(\frac{p_i(a_b) - p_i(a_j)}{\Delta o_i}\right)^2}. \quad (2)$$

For all confidence parameters $\Psi \leqslant 1$, the predicted RSL for a specific Earth model $p_i(a_j)$ fits the observational data as well as that of the best-fit Earth model $p_i(a_b)$ within the 1σ uncertainty.

4. Results and discussion

4.1. Tectonic movements

In the Belgian coastal plain, palynologically dated Eemian highstand deposits occur at a very shallow depth of about 1–2 m below present-day MSL (e.g. Paepe et al., 1972; Mostaert and De Moor, 1984, 1989). As they were deposited around 125 ka BP (pollen zone E4b or beginning of E5), this translates to an average, linear tectonic subsidence rate of only 0.008–0.16 m/ka. In the western Netherlands, Eemian highstand deposits are found at

greater depths and exhibit more altitudinal variability than in Belgium (e.g. Bosch et al., 2000). Their highest occurrence is in the Eemian-type locality in Amersfoort (Cleveringa et al., 2000). Using the Eemian sea-level curve established by Zagwijn (1983) for this area, Eemian highstand deposits occur at about 9–10 m below present-day MSL and imply a tectonic subsidence rate of 0.072–0.08 m/ka. These subsidence rates agree reasonably well with those obtained from Kooi et al. (1998) using the backstripping technique, which amount to ca 0.05 m/ka for Zeeland and ca 0.1 m/ka for the western Netherlands. However, Kooi et al. (1998) show that higher values of 0.12–0.17 m/ka apply towards the northwest of the country (Noord-Holland). Thus, the Eemian data from Amersfoort probably reflect a lower limit for the average tectonic subsidence rate which should be assumed for the western Netherlands data set, and it seems appropriate to work with a maximum value of ~0.15 m/ka instead. The maximum tectonic subsidence component of the western Netherlands relative to Belgium is thus set at 0.142 m/ka in this paper (0.15 minus 0.008 m/ka).

The highest occurrence of Eemian highstand deposits along the northwest German coast is found at 6.4 m below present-day MSL to the south of the Frisian Island Juist (Behre et al., 1979) and 5 m below MSL in the middle of the Kiel Canal (Gripp, 1964), thus rising gradually from the west to the east. These levels translate to average northwest German tectonic subsidence rates of 0.051 m/ka for the west and ca 0.04 m/ka for the east—or a maximum tectonic subsidence component of 0.043 m/ka relative to Belgium (0.051 minus 0.008 m/ka). These values are supported by the present-day subsidence rate of <0.1 m/ka along the German North Sea coast, which was calculated from two levelling activities carried out from 1928 to 1931 and from 1949 to 1955 (Gronwald, 1960; Behre, 2003, 2007).

Estimated long-term sedimentation/tectonic subsidence rates in the North Sea vary greatly depending on the proximity to the sedimentary trough trending north–northwest down the centre of the southern North Sea. There are at least two closed basins in which maximum Quaternary thickness exceeds 1 km (Caston, 1979). Thus, an average subsidence of between 0.4 and 0.04 m/ka can be postulated, depending on the location (see Table 2).

4.2. Visual comparison of northwest European MSL data: relative isostatic subsidence

Direct relationships between sea-level data from the analysed regions using the converted MSL data of Appendix A and a number of possible eustatic sea-level curves are illustrated in Fig. 6. The MSL envelope of northwest Germany lies significantly below those of the Netherlands and Belgium between ca 10 and 4 cal. ka BP, the MSL envelopes diverging progressively back in time. This pattern of divergence becomes even clearer when hypothetical MSL curves are drawn through the mid-lines of the respective MSL error bands (Fig. 6 inset). There is still much discussion on the exact magnitude and timing of delivery of glacial meltwater to the global ocean (i.e. the eustatic signal), which has been inferred from sea-level observations and modelling procedures in both far-field and near-field regions in a number of studies, but without great consensus (see Fig. 6). At far-field locations, the RSL signal is commonly characterised by a mid-Holocene sea-level maximum, or highstand, between approximately 7 and 6 cal. ka BP, when meltwater production greatly decreased (e.g. Pirazzoli and Pluet, 1991). A subsequent fall in sea level from this time to the present is associated with ongoing GIA processes, i.e. hydro- and glacio-isostatic loading. Reconstructions of the amount of global melt from this highstand time onwards varies between 1.5 and 2 m (Nakada and Lambeck, 1989), 3 m (Lambeck and Bard, 2000; Lambeck, 2002), 3 and 5 m (Fleming et al., 1998) or a value of a few metres up to ca 4 cal. ka BP, with no discernable global melt from this time to the present (Peltier, 2002; Milne et al., 2005). The Belgian MSL envelope shows the best general fit with eustatic sea-level rise, at least with the composite sea-level curves of Fleming et al. (1998), but still lies significantly below them from ca 7 cal. ka BP onwards. Indeed, Lambeck (1997) already showed that sea-level change further to the south along the French Atlantic and Channel coasts is characterised by considerable spatial variability because of the continuing effects of glacio- and hydro-isostasy on these further regions. Nevertheless, the comparison of our northwest European data shows that tectonic and/or isostatic crustal movements have had the smallest net effect on the altitude and position of the Belgian coastal plain during the Holocene. The large altitudinal differences between the Belgian MSL curve and the MSL curves of the Netherlands, northwest Germany and the southern North Sea show that the latter areas have clearly subsided relative to Belgium between 10 and 4 cal. ka BP. As eustatic sea-level rise is assumed to be a constant factor for all areas, and the tectonic subsidence components between the areas under consideration (Section 4.1) reveal that tectonic movements contribute only very little to the total difference in RSL between these regions, the observed variability must have a mainly isostatic origin.

By subtracting the maximum tectonic component from the total differential crustal movement between Belgium and the western Netherlands using the methods described in Section 3.2, Kiden et al. (2002) were already able to show that the western Netherlands and the southern North Sea have undergone considerable isostatic subsidence relative to Belgium during the Early and Middle Holocene. These authors used MSL curves which were based only on the more reliable positions of the youngest/lowest MSL data points of both areas. However, when our MSL data, derived from upper limit of MSL as well as local MHW data and exhibiting significantly larger error bars, are treated in the same manner, we find that the upper range of the western Netherlands MSL band consistently plots within the lower range of the Belgian MSL band since ca

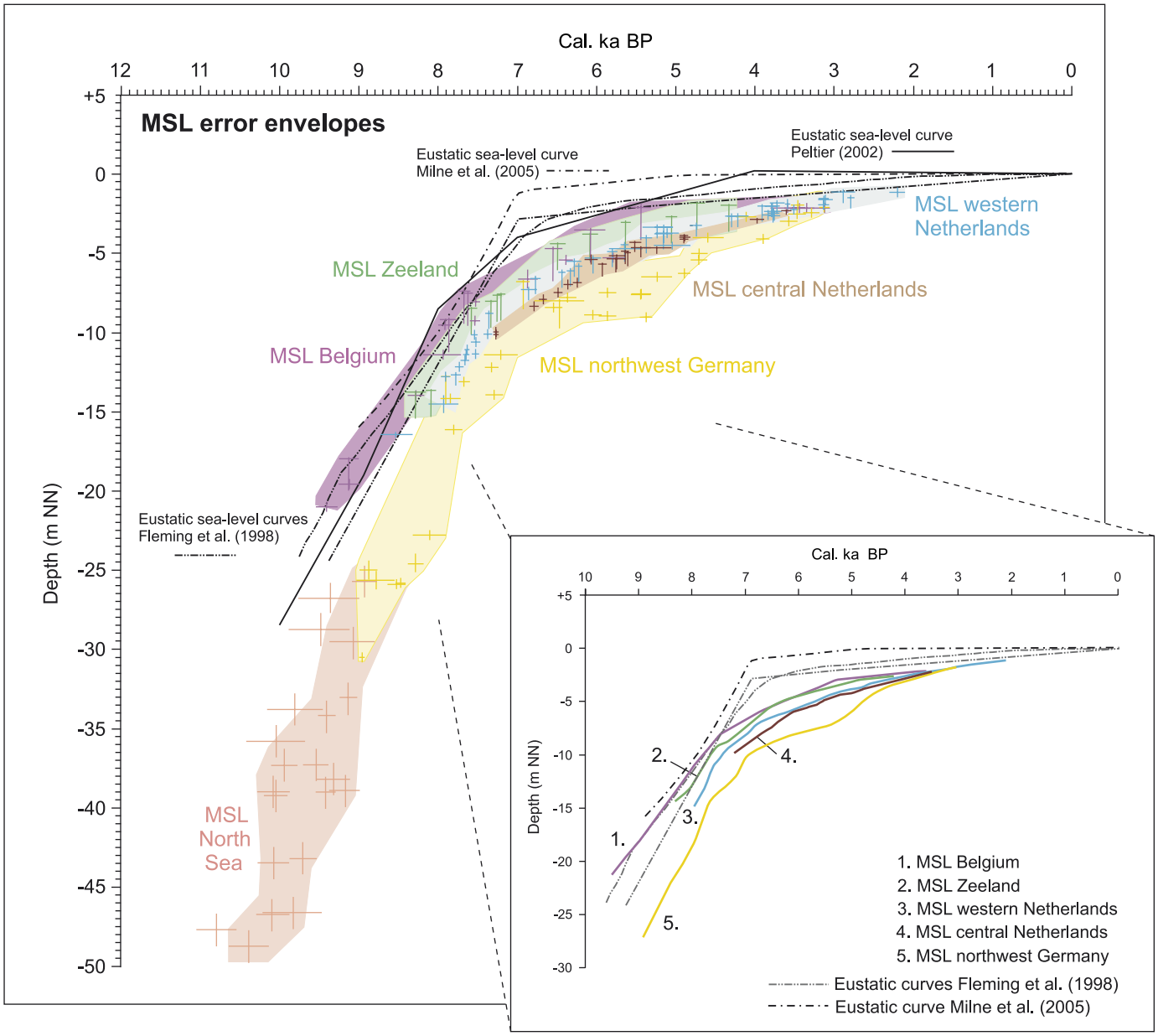

Fig. 6. Error bands of estimated MSL (determined from the local MHW/upper limit of MSL data as outlined in Section 3.1 and Appendix A) of Belgium, the Netherlands, Germany and the southern North Sea in comparison with the eustatic sea-level curves of Fleming et al. (1998), Peltier (2002) and Milne et al. (2005). The MSL curves depicted in the inset represent the mid-lines of the respective MSL error bands.

7 cal. ka BP (Fig. 7). Strictly speaking, the isostatic subsidence of the western Netherlands relative to Belgium may thus have been smaller than that predicted by Kiden et al. (2002). In reality, it is clear that our MSL data are probably biased by an overcorrection resulting from the use of large present-day (Belgian) tidal ranges, and the interpreted MSL curves used by Kiden et al. (2002) are likely to be more accurate than the data used to construct them, as is done here.

Interestingly, the MSL error bands of Belgium and northwest Germany show no overlap until ca 4.8 cal. ka BP when they finally converge, even after subtraction of the maximum tectonic component between the two areas (Fig. 7). This means that even when large present-day tidal ranges are used for correction to MSL, which most likely leads to an underestimation of isostatic subsidence as shown by the Belgian–Dutch data set, there is still no overlap between the MSL error bands of the two areas from 9 to 5 cal. ka BP. Thus, contrary to the belief that the German North Sea coast has remained tectonically and isostatically stable during the Holocene (e.g. Behre, 2003, 2007), these comparisons show that the northwest German coast has indisputably undergone considerable isostatic subsidence during the last 10 cal. ka BP. Assuming that tectonic activity has been adequately corrected for, we can tentatively provide a rate of isostatic subsidence relative to Belgium of ca 7.5 m over the last 8 cal. ka BP for northwest Germany and ca 2.5 m over the same time

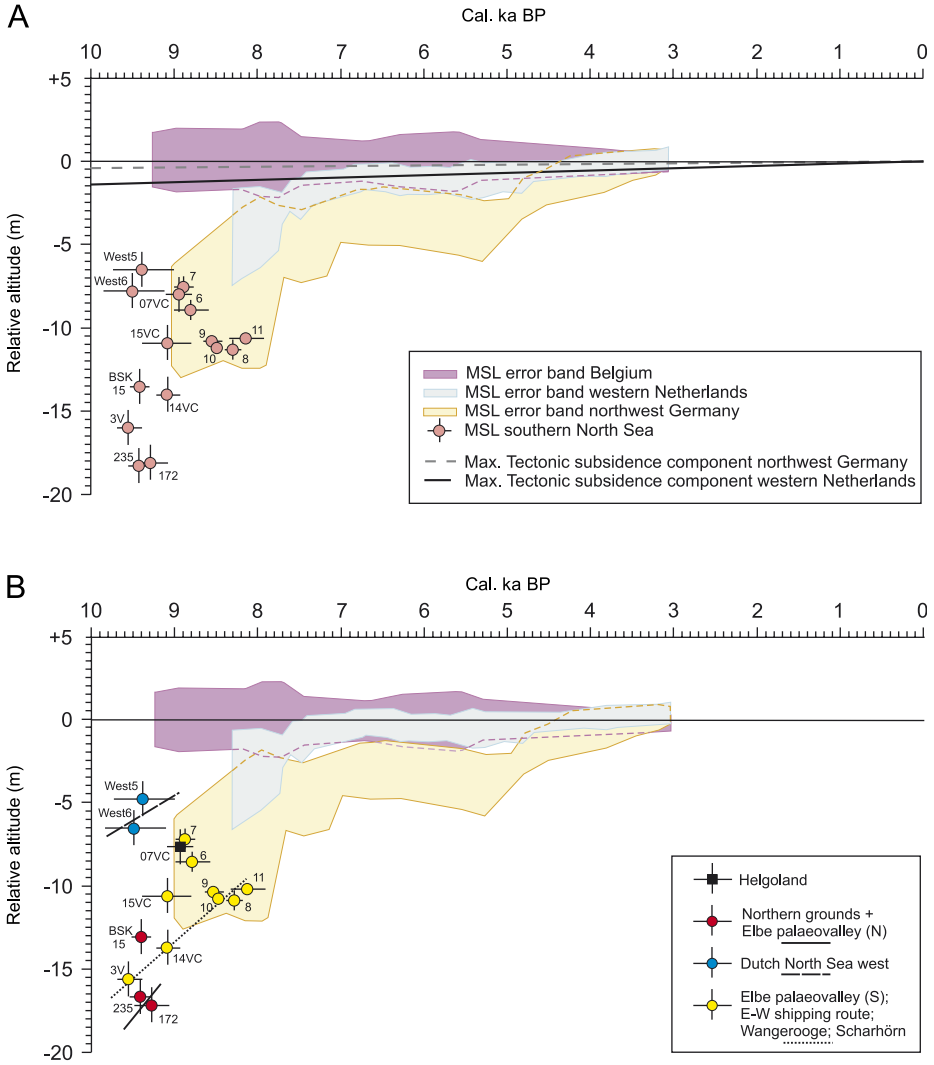

Fig. 7. Differential crustal movements between Belgium, the western Netherlands, northwest Germany and several positions in the southern North Sea based on relative altitudinal differences between MSL error bands/index points. (A) Total differential crustal movement, and (B) minimum isostatic component after the estimated maximum long-term tectonic subsidence component (determined from Eemian sea-level highstand data; see Sections 3.2 and 4.1) between regions has been subtracted from the total differential movement. Note the significant overlap between the Belgian and western Netherlands MSL error bands, whereas northwest Germany shows a discrete isostatic subsidence component relative to Belgium before 4.8 cal. ka BP. The isostatic subsidence components of the southern North Sea samples are, in the absence of suitable younger tectonic data, based on the subtraction of estimated mean Quaternary subsidence rates from the total differential crustal movement (Section 4.1).

interval for the western Netherlands. Translated to relative rates of subsidence, we reconstruct a gradual decay of ~2.67 m/ka (NL) and ~3.33 m/ka (D) for the period 9–7.5 cal. ka BP, ~0.4 m/ka (NL) and ~1.2 m/ka (D) for the period 7.5–5 cal. ka BP, and an almost negligible value (NL) and ~0.4 m/ka (D) since 5 cal. ka BP.

The heights of several sea-level index points from the southern North Sea are also illustrated in relation to the Belgian curve in Fig. 7A. Unfortunately, the absence of Belgian sea-level data before 9.4 cal. ka BP means that relationships with older North Sea samples cannot be analysed. Nevertheless, the sea-level index points around 9 cal. ka BP illustrate how variable the crustal movements between the southern North Sea and Belgium have been: sample 07VC from Helgoland and samples 5 and 6 from the western Dutch North Sea show a total differential crustal movement of only ca 8 m with respect to Belgium; samples 14VC from the E–W shipping route and 3V from the southern Elbe palaeovalley, however, show a difference of ca 14 m and samples 235 and 172 from the northern Elbe palaeovalley and Northern grounds (near the border with the Danish North Sea sector) demonstrate huge altitude differences of ca 18 m. Using the average Quaternary sedimentation rates from these locations as an approximate measure of long-term tectonic subsidence (Table 2), the tectonic and hence the isostatic component with respect to Belgium can be roughly estimated (Fig. 7B). The emerging isostatic component of the total differential crustal subsidence between Belgium and the southern North Sea shows only a slight decrease from our northernmost positions 235 and 172 to those located closer to the German coastline in the southern Elbe palaeovalley and

offshore Wangerooge and Scharhörn, which in turn have not actually experienced very much more isostatic subsidence than the northwest German coastal samples themselves. In contrast, the isostatic component of subsidence of the western Dutch North Sea has been significantly smaller (ca 8 m less than that of the German Bight at 9.5 cal. ka BP). We must, however, bear in mind that these values are rough predictions only and not based on suitably young (Holocene) tectonic subsidence data, which may well deviate from those taken to represent the Quaternary as a whole (e.g. Kiden et al., 2002; section 5.1 of this paper).

Despite the uncertainties involved we believe that the relationships described above provide additional evidence for the original inference made by Kiden et al. (2002) that the amount of glacio-isostatic subsidence decreases strongly in a southwesterly direction through northwest Europe and with time. The data are in agreement with the idea of Holocene subsidence of the so-called peripheral glacial forebulge around the Fennoscandian ice sheet or zone of glacio-isostatic rebound, which was previously reconstructed from both model and observational data and is assumed to have been centred in the North Sea between Norway and Great Britain, extending through northwest Netherlands and northern Germany (e.g. Fjeldskaar, 1994; Lambeck, 1995). In fact, our area of strongest relative isostatic subsidence around the northern Elbe palaeovalley and the Northern grounds could well lie close to the centre of the bulge, as a more northerly position would conflict with the position of the present-day axis of tilting which runs through Jutland in Denmark. Alternatively, the slightly deeper positions of the lowermost German North Sea data in comparison to the northwest German coastal data in Fig. 7B may well have been caused by a stronger hydro-isostatic subsidence component in these offshore areas, resulting from sediment and water loading in the North Sea. While generally smaller in amplitude than the ice-load contribution, its spatial variability is considerably greater, its magnitude being dictated mainly by coastline symmetry (i.e. increasing subsidence perpendicular to the coastline). Johnston (1995) was able to show that meltwater models that do not take account of hydro-isostatic processes produce errors in predictions of sea-level change of up to 10 m at 10 cal. ka BP along the east coast of England and along the southern edge of the North Sea. However, a relatively high hydro-isostatic component of ca 5 m at 9 cal. ka BP at the Northern grounds and ca 3 m in the German near-coastal areas would be required to create a similar glacio-isostatic component of subsidence throughout the entire German North Sea and coastal area. It is unclear from the relatively scarce observational data from the northern and northwest Netherlands, and North Sea locations such as the Dogger Bank and Oyster grounds, whether these locations should be included in the zone of maximum Post-Glacial forebulge subsidence or not. Modelling of RSL in these regions provides better constraints on the possible southward extension of the area of maximum forebulge subsidence (see Section 4.4).

4.3. Model results: radial viscosity structure of the mantle

A parameter search of data sets (with and without correction for compaction) has been carried out in order to determine the best-fit Earth models (i.e. values for lithosphere thickness, upper-mantle viscosity, lower-mantle viscosity) which best explain the RSL variation in each of our analysed areas (results are summarised in Table 1). The following patterns become evident (Fig. 8):

Belgium: The 1σ confidence range of possible Earth parameters fitting the Belgian RSL data set is shown in the parameter space by the light-grey shading in Figs. 8A and B. The best-fit Earth model (triangle) has a lithosphere thickness $H_l = 140$ km, an upper-mantle viscosity $\eta_{UM} = 2 \times 10^{21}$ Pa s and a lower-mantle viscosity $\eta_{LM} = 2 \times 10^{22}$ Pa s. The misfit for this model $\chi = 2.31$. The values for all three parameters are not well constrained. Notably, lithosphere thickness varies over the total range of parameter values ($H_l \in [60, 160]$ km), and upper-mantle viscosity varies over the range ($\eta_{UM} \in [4, 30] \times 10^{20}$ Pa s). The large confidence areas and the good fit of several different Earth models to the data set are a consequence of the spatial and temporal distribution of the Belgian RSL data (Fig. 6), which of all our RSL data show the best general fit with eustatic sea-level signals and thus to a large extent tend to trace the ocean model. Hence, the data are not very sensitive to the Earth's interior structure and additionally too far away from former ice sheets (British Isles and Scandinavia) to allow a better determination of the Earth's structure beneath Belgium with this method.

The Netherlands: The best-fit Earth model for this data subset (stars in Figs. 8A and B) is characterised by a lithosphere thickness $H_l = 100$ km, and upper-and lower-mantle viscosities $\eta_{UM} = 7 \times 10^{20}$ and $\eta_{UM} = 7 \times 10^{21}$ Pa s, respectively. The misfit for this model $\chi = 2.40$. Lithosphere thickness as well as the upper-mantle viscosity are better constrained than for Belgium, with permissible ranges limited to $H_l \in [65, 130]$ km and $\eta_{UM} \in [7, 10] \times 10^{20}$ Pa s, respectively (within the dark-grey shading in Fig. 8). Lower-mantle viscosity is also relatively well constrained at $\eta_{LM} \in [3, 9] \times 10^{21}$ Pa s.

Northwest Germany: The best-fit Earth model for the German data subset (diamonds in Figs. 8A and B) is characterised by a lithosphere thickness $H_l = 80$ km, and upper- and lower-mantle viscosities $\eta_{UM} = 7 \times 10^{20}$ and $\eta_{LM} = 7 \times 10^{21}$ Pa s, respectively. The misfit for this model $\chi = 2.36$. The range of permitted lithosphere thickness values is $H_l \in [60, 95]$ km and that of upper-mantle viscosity is $\eta_{UM} \in [6.5, 9] \times 10^{20}$ Pa s (within the dark-grey shading in Fig. 8). Lower-mantle viscosity is relatively well constrained at $\eta_{LM} \in [4, 10] \times 10^{21}$ Pa s. Thus, the best-fit Earth parameters and the allowable parameter ranges for northwest Germany and the Netherlands are very similar

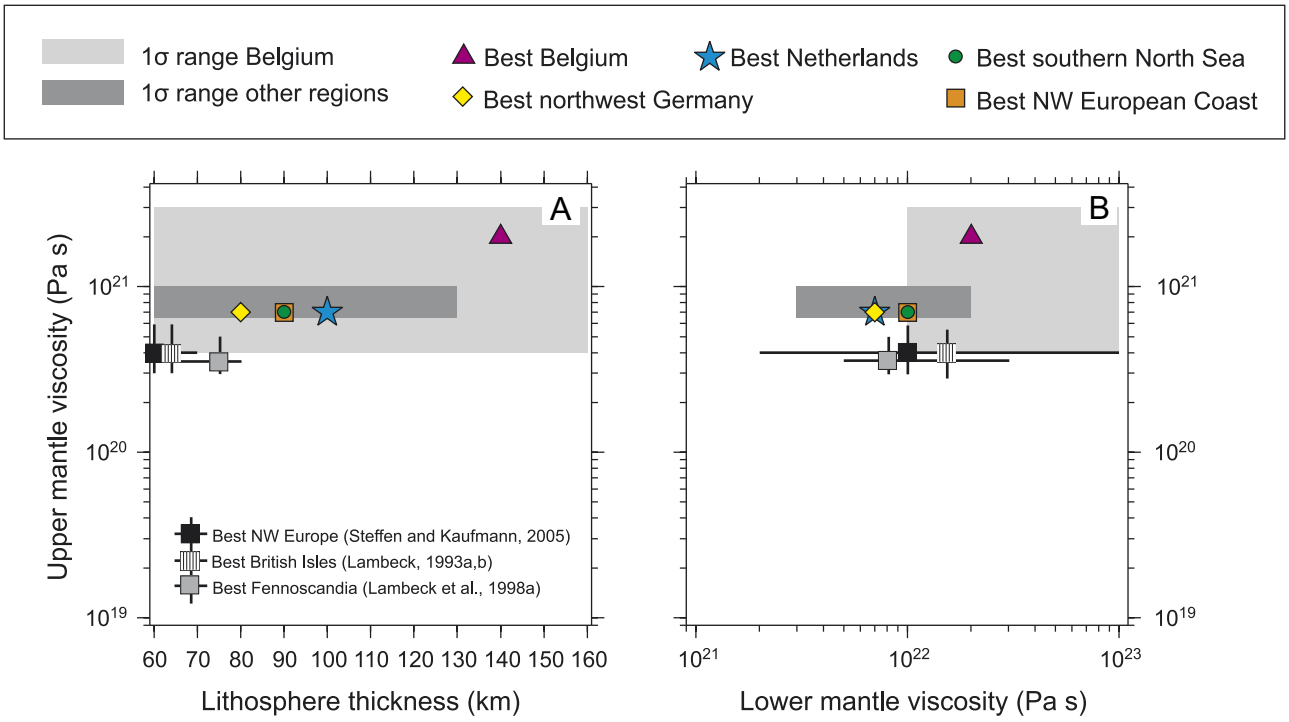

Fig. 8. Best regional three-layer Earth models (marked with symbols) and the confidence regions $\Psi \leqslant 1$ for NW European RSL data sets using the ice model RSES. Belgium: light-grey shading; other NW European regions: dark-grey shading. (A) RSL data as a function of lithospheric thickness and upper-mantle viscosity for a fixed lower-mantle viscosity of 2×10^{22} Pa s for Belgium, 7×10^{21} Pa s for the Netherlands, 7×10^{21} Pa s for Germany, 10^{22} Pa s for the North Sea and 10^{22} Pa s for Europe, and (B) RSL data as a function of upper- and lower-mantle viscosities for a fixed lithospheric thickness of 140 km for Belgium, 100 km for the Netherlands, 80 km for Germany, 90 km for the North Sea and 90 km for Europe. Comparisons with published best-fit Earth models are shown.

Table 1
Three-layer Earth models

	H_l (km)	η_{UM} (10^{20} Pa s)	η_{LM} (10^{20} Pa s)	X (NC)	X (WC)
Search range	60–160	0.1–40	0.1–10		
Data set	RSES				
Belgium	60–160 (140)	4–30 (20)	1–10 (2)	2.31	2.09
Netherlands	65–130 (100)	7–10 (7)	0.3–0.9 (0.7)	2.40	2.40
Northwest Germany	60–95 (80)	6.5–9 (7)	0.4–1 (0.7)	2.36	2.26
Southern North Sea	80–95 (90)	6.5–10 (7)	0.7–2 (1)	2.49	2.49
NW Europe coast	60–110 (90)	7–10 (7)	0.7–1.5 (1)	2.45	2.37

Free parameters are lithospheric thickness H_l, upper-mantle viscosity η_{UM}, and lower-mantle viscosity η_{LM}. χ is the misfit for the best three-layer Earth model. Results for the three-layer Earth models fitting the NW European RSL data within the 1σ-uncertainty range are shown for different data sets, with the best-fit Earth models indicated between brackets. NC = no compaction correction; WC = with compaction correction.

except for the best-fit value of lithospheric thickness (80 vs. 100 km, respectively). The German value of 80 km is the lowest of all analysed data sets.

Southern North Sea and NW Europe: The best-fit Earth models for the southern North Sea and for NW Europe as a whole are identical (circles and squares in Figs. 8A and B) and reveal a lithosphere thickness $H_l = 90$ km, an upper-mantle viscosity $\eta_{UM} = 7 \times 10^{20}$ Pa s and a lower-mantle viscosity $\eta_{LM} = 10^{22}$ Pa s. The misfit for this model $\chi = 2.49$ for the North Sea and $\chi = 2.45$ for NW Europe. The highest misfit of all regions is provided by the North Sea samples, which is not surprising considering the large spatial and temporal distribution of the data set in a basin which has been influenced by variable crustal movements associated with both tectonic and isostatic activity (Section 4.2). Nevertheless, focussing on the 1σ confidence range (Table 1), lithosphere thickness is much better constrained than for the Netherlands and northwest Germany ($H_l \in [80, 95]$ km), and upper-mantle viscosity is similar ($\eta_{UM} \in [6.5, 10] \times 10^{20}$ Pa s). The similarity between the best-fit Earth models for the southern North Sea and NW Europe shows that the index points of the former govern the selection of the best-fit Earth model for the latter, although a slightly better misfit is achieved by using

the large amount of coastal data. Altogether, the North Sea RSL data set appears to be more sensitive to Earth structure than the other RSL data sets. Additionally, the index points are (i) closer to the former ice sheets (British Isles and Scandinavia), and (ii) derived from deeper parts/older deposits than most of the indicators from the other data sets. This allows a better determination of the Earth's structure beneath the southern North Sea region.

Focussing only on the three main continental regions Belgium, the Netherlands and Germany, the thickness of the lithosphere is determined to be around 140 km under Belgium, and then decreases to a thickness of ca 100 km under the Netherlands and ca 80 km along the northwest German coast, although we must bear in mind that the 1σ ranges of possible lithosphere thicknesses are considerably larger in all areas (Table 1). Nevertheless, the results are in accordance with a decreasing lithosphere thickness towards the British Isles (60–70 km; Lambeck, 1993a,b; Steffen and Kaufmann, 2005) and Fennoscandia (60–80 km; Lambeck et al., 1998a); see Fig. 8 for a comparison. Upper-mantle viscosities for all our analysed regions except Belgium are around $\eta_{UM} = 7 \times 10^{20}$ Pa s, and cover a relatively narrow range between $\eta_{UM} \in [6.5, 10] \times 10^{20}$ Pa s. Compared to the results of Fennoscandia (Lambeck et al., 1998a), the British Isles (Lambeck, 1993a,b) and the reduced set of NW European RSL data from Steffen and Kaufmann (2005), who all report upper-mantle viscosities of $[3, 6] \times 10^{20}$ Pa s, our values are slightly higher. The NW European results of Steffen and Kaufmann (2005) are, however, based more on data from the British Isles than from NW Europe, and so there is only an overlap of a few western Netherlands index points between both studies. The variability in lithosphere thickness and upper-mantle viscosity across NW Europe and Fennoscandia shows that the response of the upper mantle to the changing ice and water loads across the region is spatially more heterogeneous than suggested previously (e.g. Lambeck et al., 1998a). Lower-mantle viscosity is not very well constrained and the values are comparable in all of the data sets, confirming the low resolving power for lower-mantle viscosity of RSL data with a relatively small spatial distribution.

A parameter search of data sets in which possible effects of compaction have been taken into account shows that the correction for compaction does not lead to the choice of a different best-fit Earth model in any of our five sub-regions, although a significant decrease in the misfit was obtained in the Belgian, northwest German and hence the NW European data sets. The misfit for the Belgian model is $\chi = 2.31$ without a compaction correction and $\chi = 2.09$ with the correction, an improvement of 10%. This improvement of the misfit occurs due to an even better general fit with the ocean model. Despite the improved misfit, the altitude correction for compaction was obviously too small to allow a clearer determination of a reliable Earth model for this region. The misfit for the northwest German model is $\chi = 2.36$ without the compaction correction and $\chi = 2.26$ with the correction, an improvement of only 4%. Again, this decrease in the misfit is probably due to a slightly better fit with the ocean model. As a result of the misfit improvement in the Belgian and German data sets, the misfit for the NW European data set also decreases from $\chi = 2.45$ without the compaction correction to $\chi = 2.37$ with the correction (3% improvement). However, despite the decreases in the misfit, the consideration of compaction did not help to better isolate specific Earth models.

4.4. Predicted RSL curves: constraining the region of maximum Post-Glacial isostatic subsidence in NW Europe

The ice and Earth models described in the previous section produce predicted RSL curves for NW Europe which correlate well with the sea-level observational data (i.e. misfit values are low), thus implying that the models are good enough to predict RSL change for any arbitrary location within the analysed region (e.g. in areas where we have no observational data) as long as we are constantly aware of the assumptions and limitations on which they are based (Section 3.3). The actual error limits of the model results are greatly dependent on the 1σ uncertainty of the best-fit Earth model, which is different for each of our previously defined sub-regions. The total model error band was calculated to be ± 0.5 m from the Early to Middle Holocene in the southern North Sea, the error becoming significantly smaller with decreasing age towards the present. Slightly higher error bands of up to ± 1 m are postulated for the German coastal locations during the Early Holocene. Fig. 9 summarises predicted RSL for 24 selected locations across the region. For each location the best-fit regional Earth model was used to calculate the RSL curve over the last 10 ka. A clear distinction is made between RSL in the Belgian and Zeeland areas (nrs 1–5), RSL in the western and central Netherlands (nrs 6–10) and RSL in the remaining regions, although the general pattern is one of quasi-continuous drop in relative altitude from the southwest to the northeast of the analysed area (i.e. an increasing net effect of Post-Glacial isostatic adjustment/subsidence towards the Fennoscandian landmass). However, the RSL curves from western Schleswig-Holstein (nrs 14 and 15) plot higher than those of the more southerly positions Wilhelmshaven (nr 16) and Cuxhaven (nr 17), which in turn plot higher than those from the southern North Sea in which an influence of hydro-isostatic processes in addition to glacio-isostatic subsidence is likely. As coastal locations have not been influenced very strongly by hydro-isostatic processes, a zone of maximum glacio-isostatic subsidence (i.e. the position of the centre of the peripheral glacial forebulge) can be estimated to run in a relatively narrow band through northwest Germany in the regions of the Jadebusen, Weser and Elbe Estuaries (stippled zone in Fig. 9), but not including the coast of Schleswig-Holstein. Its extension into the southern North Sea is masked by increasing hydro-isostatic processes and can only be roughly estimated. Nevertheless, assuming that

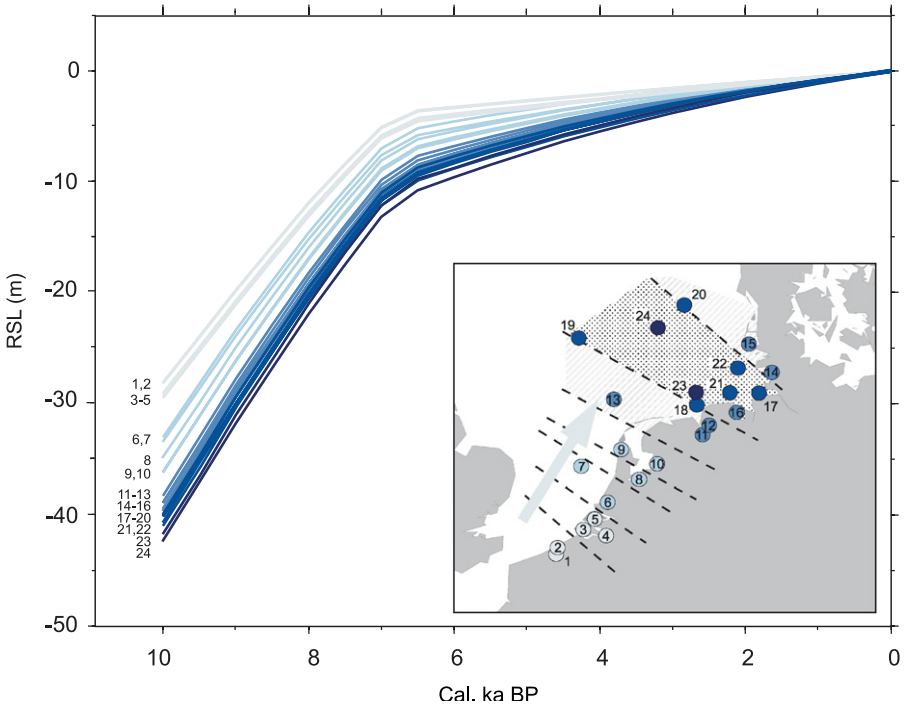

Fig. 9. Predicted smooth RSL curves based on regional best-fit Earth models for 24 locations in NW Europe, showing a quasi-continuous drop in RSL altitude from the southwest to the northeast of the analysed area. Stippled area = approximate zone of maximum Post-Glacial forebulge subsidence; striped area = peripheral zone of strong forebulge subsidence. → 1 = Dijk; 2 = Westende; 3 = Ritthem; 4 = Berendrechtsluis; 5 = Anna Jacoba polder; 6 = Hillegersberg; 7 = Dutch North Sea west; 8 = Almere; 9 = Den Helder; 10 = Schokland; 11 = Winschoten; 12 = Hatzum; 13 = Oyster grounds (Dutch North Sea); 14 = Tiebensee; 15 = Föhr; 16 = Wilhelmshaven; 17 = Cuxhaven; 18 = Juist; 19 = Dogger Bank; 20 = Northern grounds; 21 = Wangerooge; 22 = Helgoland; 23 = E–W shipping route and 24 = northern Elbe palaeovalley.

the sites at the northern Elbe palaeovalley (nr 24) and the Northern grounds (nr 20) have experienced a comparable hydro-isostatic subsidence to that at the Dogger Bank (nr 19), the significantly lower RSL position of nr 24 indicates that this relatively northward location must still have been situated within the region of maximum forebulge subsidence (Fig. 9). However, a drop in subsidence is observed up to the more northerly position of nr. 20. The striped zones in Fig. 9 indicate peripheral areas of slightly lower, though still strong, glacio-isostatic subsidence. The northern extension cannot be determined using our data; the southern extension, however, runs southward of the Oyster grounds (nr 13) and through the northern Netherlands (nr 11). However, the central and northwest Netherlands, and all locations further to the south, have clearly been affected by significantly less glacio-isostatic subsidence.

It is important to note that the relatively large predicted difference in RSL between different locations of the German data set (e.g. approximately 2 m at 10 cal. ka BP between Hatzum (nr 12) and Wangerooge (nr 21)) reflects—independent of the model error band—the highly variable influence of forebulge subsidence on these sites and denotes that the data of the German sea-level curve of Behre (2003, 2007) cover a geographic area too large to be summarised into a single curve. More local sea-level curves are required in order to reinterpret the nature and extent of the regressional phases which Behre (2003, 2007) describes for the entire length of the German North Sea coast.

5. Comparison between observational and modelled sea-level curves: some examples

Comparisons between observational and modelled RSL data within a local area may allow the identification of "outlier" sea-level index points, which in turn can provide important information on local effects such as tectonic subsidence/uplift, compaction and/or possible past changes in tidal range (e.g. Shennan et al., 2000a). Determining the relative importance of each of these local factors on altitude discrepancies is difficult, especially considering the fact that they may have acted simultaneously. In areas such as the central Netherlands where sample compaction was not considered to be a problem (Van de Plassche et al., 2005), tectonic activity has been low (Kooi et al., 1998) and tidal ranges are low enough (0.2–0.8 m: Van de Plassche, 1995) to mask the uncertainties involved in calculating MSL from local MHW and MSL data, sea-level index points actually show an excellent fit to the predicted RSL curve (Fig. 10A). However, such a good relationship is an exception rather than the general trend of the data set. A careful examination of the residuals (= difference between observed and predicted RSL values) can help to elucidate potentially important factors, and we

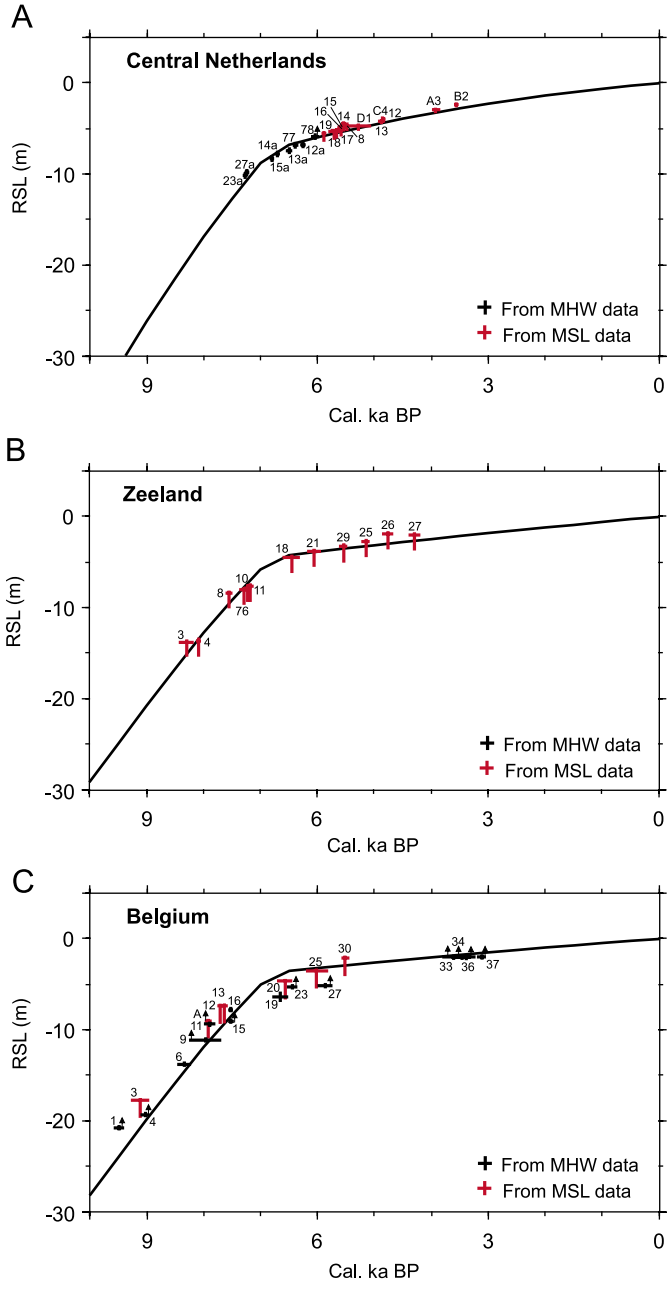

Fig. 10. Comparisons between observational and predicted RSL data for the (A) central Netherlands, (B) Zeeland and (C) Belgium. Predicted RSL curves are based on regional best-fit Earth models and reflect the situation at one particular location only (i.e. do not indicate small within-region variations in RSL). Discrimination between data derived from local MHW data and those derived from upper limit of MSL data has been made. Samples in which some compaction may be expected are marked by an upward arrow.

would like to briefly discuss some examples, including the constraints involved, below.

5.1. Past changes in tidal range?

Calculated MSL ranges derived from local MHW or upper limit of MSL data are biased mainly by the underlying assumption that tidal ranges have not changed significantly during the last 10 ka, although there is often no direct evidence that this is the case. Thus, it is important to decipher whether such an assumption holds for a particular area or not. We provide one example of a data set in which the use of large present-day tidal ranges for the calculation of past MSL appears warrantable (Belgium and Zeeland), and one example in which it does not (Emden/Hatzum, i.e. along the Dutch/German border).

For the Belgian and Zeeland data sets (which were bundled for modelling purposes), the 1σ confidence range of possible Earth parameters fitting the MSL data is large and so the choice of the best-fit Earth model may be considered to be more arbitrary. Nevertheless, the best-fit predicted RSL curve closely fits the MSL data from Zeeland (Fig. 10B), and shows a good though more variable fit with the MSL data from Belgium (Fig. 10C). Here, discrepancies between observed and modelled data are generally positive (i.e. predicted MSL lies lower than observed MSL), especially between 10 and 7 cal. ka BP. The residuals cannot be explained by tectonic uplift, which has been almost negligible and negative since the Last Interglacial highstand (Section 4.1). Sea-level independent peat growth is also highly unlikely, especially for the data derived from the tops of peats in which a marine contact was present (= local MHW data). When the Zeeland MSL data do indeed represent actual MSL, as predicted from both intensive geological analysis (Kiden, 1995) and the best-fit Earth model (Fig. 10B), then the trend shown by the Belgian data indicates that the sea-level data have not at all been overcorrected to MSL due to the use of present-day high coastal tidal amplitude (~2 m). In fact, the data suggest that tidal ranges may even have been somewhat higher here during the Early Holocene. These results support those of Roep and Beets (1988), who reconstructed a slightly higher tidal range along the western coast of the Netherlands before ca 5 cal. ka BP. Thus, high tidal ranges similar to those at the present probably developed directly after the connection of the North Sea to the English Channel occurred in response to rapid sea-level rise at ca 9 cal. ka BP (e.g. Beets and Van der Spek, 2000; Shennan et al., 2000b; Van der Molen and de Swart, 2001). Additional conclusions which may be drawn from Fig. 10C are that (i) the local MHW data of Belgium most likely reflect contemporaneous coastal MHW (i.e. minimal floodbasin effect); and (ii) the older upper limit of MSL data from Belgium (>7 cal. ka BP) formed well above contemporaneous MSL, most likely around (coastal) MHW level. These findings are corroborated by the results of Van de Plassche (1995) who found that the onset of significant tidal dampening in the Netherlands west-central intra-coastal area and Rhine–Meuse Delta only occurred at ca 6.4 cal. ka BP, the Rotterdam curve (including the "donk" index points in Appendix A) approximating the rise of coastal MHW before that time.

A clearly lower past tidal range is reflected by the sea-level data of Emden/Hatzum (Fig. 11A), which are derived

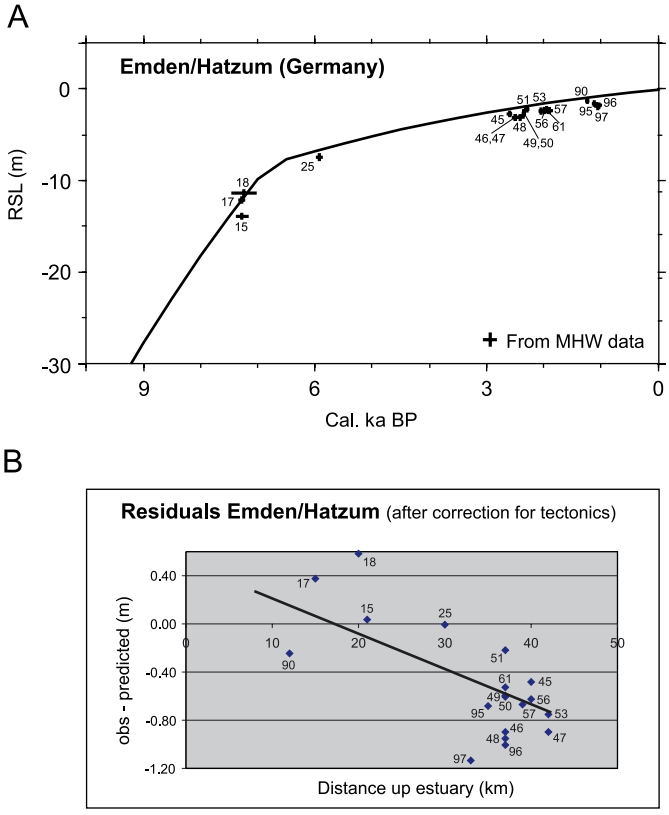

Fig. 11. (A) Comparison between observational and predicted RSL data for Emden/Hatzum (Dutch/German border). The predicted RSL curve is based on the regional best-fit Earth model and reflects the situation at one particular location only (i.e. does not indicate small within-region variations in RSL). (B) Relationship between observed-model RSL differences (residuals) and sample distance up the Ems estuary (km).

from the Ems River Estuary where tidal ranges at present vary between 2.6 and 3 m. Even after an upward correction for an average tectonic subsidence rate of 0.053 m/ka based on Eemian sea-level highstand data (Section 4.1), which was not accounted for in the model, most observational index points still lie below the predicted RSL curve by, on average, about 0.55 m. As compaction effects were assumed to be negligible by the original authors (see Behre, 2003), this discrepancy can only be explained by an overcorrection to MSL from local MHW data using present-day tidal ranges. Furthermore, when the residuals are compared to the distance up the estuary (e.g. Shennan et al., 2000a), we see that the discrepancies increase with increasing distance from the coast (Fig. 11B). Thus, it appears that tidal dampening occurred upstream at least until 1 cal. ka BP, with reconstructed tidal ranges varying from ca 3 to 3.5 m in the outer estuary to only about 0.5–1 m in the inner estuary. Differences occurring between samples of the same upstream distance may be due to differing bathymetries, local tectonics, consolidation or sea-level-independent peat formation. High present-day tidal ranges in the inner estuary are probably the result of deepening and narrowing of the Ems River and estuary for navigation purposes during the last 150 y.

These comparisons between observational and modelled sea-level data help to decipher where past changes in tidal range (including those caused by estuary, floodbasin and/or river effects) may be expected. As a consequence, RSL curves can be adapted accordingly, thus improving their quality and significance for future comparative and modelling purposes.

5.2. Estimation of Holocene tectonic activity in the southern North Sea

Contrary to all other data, altitude differences between southern North Sea observational and predicted MSL often exceed 1–2 m, even reaching a value of 9.41 m at the Dogger Bank (Table 2). Basal peat compaction was assumed to not have greatly affected the altitudes of the observational data. Furthermore, with the exception of the German near-coastal index points, low present-day tidal amplitudes of maximally 0.8 m were used to calculate MSL from local MHW at these sites. Thus, in the unlikely case of an even lower past tidal amplitude, the altitude difference would actually not undergo a substantial change. However, southern North Sea index points may have been lowered considerably in altitude due to tectonic subsidence (Section 4.1), which is not accounted for in the geodynamic modelling procedure. Thus, a best-fit Earth model for the southern North Sea will likely be selected which overestimates the isostatic subsidence component. Despite this attempted overcorrection of modelled MSL values, high residuals remain for several of the southern North Sea index points. Negative residual values greater than half of the observed MSL error band are considered to significantly reflect tectonic subsidence (shown by the values in bold in Table 2). For the southern North Sea samples, half of the error band (1.04 m) also corresponds to the total model error band, which was calculated to be ±0.5 m during the Early to Middle Holocene. Positive residuals might imply tectonic uplift but are more likely associated with limitations related to either the observations (e.g. peat formation above contemporaneous sea level, errors related to index point depth measurement) or the model predictions (e.g. too low MSL prediction as tectonics are not accounted for, use of one best-fit Earth model to cover a geographically extensive area). Assuming that the negative residual values have been caused mainly by tectonics, approximate values for Holocene tectonic subsidence in the southern North Sea can be calculated (Table 2). A comparison between our rough estimations of potential Holocene tectonic subsidence rates based on data-model comparisons and average Quaternary sedimentation/subsidence rates calculated from Caston (1979) suggests an approximate 2–3 times higher subsidence rate during the Holocene in comparison to the Quaternary as a whole (Table 2). One possible cause for this difference could be the uncertainty in determining the base of the Quaternary and/or the exact amount of time represented by Quaternary sediments in the North Sea (Caston, 1979).

Table 2
Rough predictions of Holocene tectonic subsidence in the southern North Sea as determined from MSL residuals

Index no.	Region	Age (cal. ka BP)	MSL obs. (m NN)	MSL error (m)	MSL pred. (m NN)	Residual (obs. − pred.) (m)	Implied tectonic uplift Holocene (m/ka)	Av. Quat. thickness (m)	Av. Quat. sed. rate (m/ka)
1	**Dogger Bank**	**9710**	**−46.6**	**±1.04**	**−37.19**	**−9.41**	**−0.97**	**700**	**0.35**
235	**Elbe palaeovalley (N)**	**9180**	**−38.88**	**±1.04**	**−35.73**	**−3.15**	**−0.34**	**350**	**0.175**
235	**Elbe palaeovalley (N)**	**9500**	**−38.98**	**±1.04**	**−37.65**	**−1.33**	**−0.14**	**350**	**0.175**
245	Elbe palaeovalley (N)	10,210	−46.7	±1.04	−46.93	0.23	0.02	300	0.12
234	Elbe palaeovalley (N)	10,210	−43.5	±1.04	−44.53	1.03	0.1	350	0.175
Gauss 1987/5	**Elbe palaeovalley (N)**	**10,890**	**−48.74**	**±1.04**	**−47.63**	**−1.11**	**−0.1**	**280**	**0.14**
172	**Northern grounds**	**9410**	**−38.18**	**±1.04**	**−36.35**	**−1.83**	**−0.19**	**200**	**0.1**
BSK VC-15	Northern grounds	9490	−34.16	±1.04	−35.51	1.35	0.14	100	0.05
BSK VC-21	Northern grounds	9950	−37.36	±1.04	−40.02	2.66	0.27	100	0.05
AU04-07-VC	Helgoland	9020	−25.73	±1.04	−28.91	3.18	0.35	<80	0.04
H15/2V	Elbe palaeovalley (S)	10,190	−39.35	±1.04	−40.87	1.52	0.15	<80	0.04
H18/3V	Elbe palaeovalley (S)	9520	−37.4	±1.04	−38.05	0.65	0.07	<80	0.04
280	Elbe palaeovalley (S)	10,210	−38.95	±1.04	−40.8	1.85	0.18	<80	0.04
HE242-14VC	E–W shipping route	9110	−32.99	±1.04	−32.81	−0.18	−0.02	<80	0.04
HE242-15VC	**E–W shipping route**	**9060**	**−29.54**	**±1.04**	**−28.47**	**−1.07**	**−0.12**	**<80**	**0.04**
2	**Oyster grounds**	**9710**	**−43.2**	**±1.04**	**−38.08**	**−5.12**	**−0.53**	**500**	**0.25**
2a	Oyster grounds	10,610	−47.7	±1.04	−48.1	0.4	0.04	1000	0.5
5	Dutch North Sea west	9410	−26.8	±1.04	−28.1	1.3	0.14	400	0.2
6	Dutch North Sea west	9520	−28.8	±1.04	−28.81	0.01	0	300	0.15
7	Dutch North Sea west	9610	−33.8	±1.04	−33.2	−0.6	−0.06	200	0.1
8	**Dutch North Sea west**	**10,210**	**−35.8**	**±1.04**	**−34.61**	**−1.19**	**−0.12**	**150**	**0.075**
6	Wangerooge	8860	−25.63	±0.58	−25.39	−0.24	−0.03	<80	0.04
7	Wangerooge	8790	−25	±0.58	−26.43	1.43	0.16	<80	0.04
8	Wangerooge	8370	−24.56	±0.58	−24.22	−0.34	−0.04	<80	0.04
9	Scharhörn	8560	−25.9	±0.3	−26.24	0.34	0.04	<80	0.04
10	**Scharhörn**	**8500**	**−25.84**	**±0.3**	**−25.41**	**−0.43**	**−0.05**	**<80**	**0.04**
11	Scharhörn	8150	−22.81	±0.3	−23.32	0.51	0.06	<80	0.04

Negative residual values greater than the half of the observed MSL error band are considered to significantly reflect subsidence and are indicated in bold in table. Large positive residuals probably reflect limitations related to both the observations (e.g. peat formation above contemporaneous sea level, error in shipboard depth measurement) and the model predictions (e.g. too low MSL prediction as tectonics are not accounted for). A comparison with average Quaternary sedimentation rates as a simplistic measure of total Quaternary subsidence (deduced from Caston, 1979) still suggests an approximate 2–3 times higher subsidence rate during the Holocene.

Another possible cause could be the use of only one best-fit Earth model for the whole southern North Sea area. However, it is promising that precisely this model is capable of reconciling both offshore and coastal data in the total NW European data set, and thus we assume that our first tentative estimates of short-term tectonic subsidence of the southern North Sea fall within the spectrum of acceptable values until more detailed surveys are carried out. Our estimated Holocene tectonic subsidence rates of between 0.1 and 1 m/ka, depending on the location, have important implications for the increasing (industrial) usage of the North Sea shelf. For example, the planning of cable routes, pipelines and wind energy plants not only requires a detailed knowledge of the shallow subsurface but is also greatly dependent on short-term subsurface stability.

The high age–depth position of the high-quality index point AU04-07-VC off Helgoland (Figs. 4 and 7) and consequently the great positive residual value between observed and expected MSL (3.18 m) is surprising as (i) its age is well constrained by one lower terrestrial and two upper tidal-flat dates (Fig. 4); (ii) shipboard depth measurement was considered to be accurate (Kudraß et al., 2004) and (iii) compaction of this thin peat (10 cm) or its Pleistocene sandy substrate can be excluded. The lowermost tidal-flat date, which was taken 40 cm above the basal peat date, is only ~200 yr younger than the peat—thus reflecting a non-erosive transition from peat to tidal-flat deposition. We suggest that the unusually high position of this basal peat reflects post-depositional uplift due to its geographical location on the edge of the Helgoland Permian salt diapir (e.g. Kockel, 1995; Baldschuhn et al., 2001). Assuming that the isostatic component has not deviated too much from values registered in the regions of the southern Elbe palaeovalley or even along the German coast, as is indeed done in the model (Fig. 9), the predicted value of MSL at a depth of 3.18 m below observed MSL at ca 9 cal. ka BP implies a post-depositional uplift of ca 0.35 m/ka associated with upward salt migration within the generally subsiding North Sea Basin. Although the indicative meaning of the two Northern grounds peats BSK VC-15 and VC-21 are less well constrained, the high positive values of their residuals also appear to be associated with their position on the flanks of a large salt diapir located slightly to the south of the sample positions (e.g. Hinz, 1968; Baldschuhn et al., 2001).

6. Conclusions

The observational and geophysical assessment of 233 previously published and five new Holocene sea-level index points from northwest Europe reveals a complex pattern of differential crustal movement between Belgium, the Netherlands, northwest Germany and the southern North Sea which cannot be solely attributed to tectonic activity. It clearly contains a non-linear, glacio- and/or hydro-isostatic subsidence component, which is small on the Belgian coastal plain but increases significantly towards the northeast in the direction of the Fennoscandian land mass. Northwest Germany, for example, has been subjected to a total isostatic lowering relative to Belgium of ca 7.5 m between 8 and 4.8 cal. ka BP, after which differential isostatic subsidence processes can no longer be unambiguously identified using a simple comparative approach. Our results confirm former investigations of Kiden et al. (2002) from the Belgian–Netherlands coastal plain and the southern North Sea and provide new evidence from more northerly regions (i.e. the German coastal and North Sea sectors) for the Post-Glacial collapse of the so-called peripheral forebulge which developed around the Fennoscandian centre of ice loading during the LGM. Furthermore, modelled RSL data suggest that the zone of maximum forebulge subsidence runs in a relatively narrow, WNW–ESE trending band connecting the German federal state of Lower Saxony with the Dogger Bank area in the southern North Sea (Fig. 9). However, sea-level data extending northwards into the Danish sector and northwestwards into the deeper parts of the North Sea are now required in order to better constrain the geographical extent and the temporal progression of (early) forebulge collapse, respectively.

Geodynamic modelling of the Earth's internal structure reveals that a broad range of Earth parameters fit the Belgian RSL data, the ranges then becoming narrower towards the southern North Sea region. In fact, the Belgian data tend to mainly trace the ocean model. Hence, the data are not very sensitive to changes in the Earth's interior structure and additionally too far away from former ice sheets (British Isles and Scandinavia) to allow a better determination of the Earth's structure beneath Belgium with this method. The models which show a best fit with the remaining RSL data predict an average lithosphere thickness of ca 90 km in northwest Europe, although a thickness of ca 100 km was reconstructed for the Netherlands and 80 km for northwest Germany. Upper-mantle viscosities for all regions except Belgium are well constrained at ca 7×10^{20} Pa s, and cover a range between $\eta_{UM} \in [6.5, 10] \times 10^{20}$ Pa s. Lower-mantle viscosities are, however, very poorly constrained, confirming the low resolving power for lower-mantle viscosity of RSL data with a small spatial distribution. These results generally confirm earlier findings of Lambeck et al. (1998a) and Steffen and Kaufmann (2005) for NW Europe but introduce a finer subdivision of differential lithosphere and mantle structure in this region. In the model predictions, no change to the best-fit Earth model selection and only a small misfit improvement of 3% were attained through the correction for compaction, which is mainly due to a better fit with the ocean model.

The comparison between modelled and observational sea-level data can provide important information on local-scale processes such as temporal changes in tidal range (e.g. negligible change in tidal amplitude along the Belgian coast, tidal dampening in the Ems Estuary) or the effects and rates of (local) tectonic subsidence (e.g. higher

Holocene tectonic subsidence in the North Sea than expected from Quaternary sedimentation rates alone). However, additional high-quality observational data are required in order to pin down more exact Earth models with a smaller variation in parameter space for each local area. Conversely, data-model comparisons will benefit greatly from the refinement of existing global ice models and the definition of more focussed regional-scale models. As such, there is still room for analytical improvement for Quaternary field geologists as well as geophysical modellers, the progress of each inevitably being linked to that of the other on a give-and-take principle which will hopefully yield fruitful results in the upcoming years.

Acknowledgements

Many thanks to Kurt Lambeck (Canberra, Australia) for providing the RSES ice model. We also sincerely thank VP Ingenieurbüro Dr.-Ing. V. Patzold for the possibility of joining their North Sea sampling cruise in May 2005, and Manfred Frechen of the Leibniz Institute for Applied Geosciences (GGA) in Hannover for conventional radiocarbon dating of the five BGR North Sea peat index points. Figs. 5 and 8 in this paper have been drawn using the GMT graphics package (Wessel and Smith, 1991, 1998). We are very grateful for the excellent reviews and numerous valuable suggestions of Patrick Kiden and Torbjörn Törnqvist, which have greatly improved this paper. The research of H. Steffen and G. Kaufmann was funded by the German Research Council (DFG research Grant KA1723-1,2).

References

Austin, R.M., 1991. Modelling Holocene tides on the NW European continental shelf. Terra Nova 3, 276–288.

Baldschuhn, R., Binot, F., Fleig, S., Kockel, F., 2001. Geotektonischer Atlas von Nordwest-Deutschland und dem deutschen Nordsee-Sektor. Geologisches Jahrbuch A 153, 3–95.

Beets, D.J., Van der Spek, A.J.F., 2000. The Holocene evolution of the barrier and the back-barrier basins of Belgium and the Netherlands as a function of late Weichselian morphology, relative sea-level rise and sediment supply. Netherlands Journal of Geosciences 79 (1), 3–16.

Behre, K.-E., 2003. Eine neue Meeresspiegelkurve für die südliche Nordsee: Transgressionen und Regressionen in den letzten 10.000 Jahren. Probleme der Küstenforschung im südlichen Nordseegebiet 28, 9–63.

Behre, K.-E., 2007. A new Holocene sea-level curve for the southern North Sea. Boreas 36, 82–102.

Behre, K.-E., Menke, B., Streif, H., 1979. The Quaternary geological development of the German part of the North Sea. In: Oele, E., Schüttenhelm, R.T.E., Wiggers, A.J. (Eds.), The Quaternary History of the North Sea. Acta Universitatis Upsaliensis, Symposia Universitatis Upsaliensis Annum Quingentesimum Celebrantis, vol. 2, Uppsala, pp. 85–113.

Bennema, J., 1954. Holocene movements of land and sea-level in the coastal area of the Netherlands. Geologie en Mijnbouw, Nieuwe Serie 16, 254–264.

Bosch, J.H.A., Cleveringa, P., Meijer, T., 2000. The Eemian stage in the Netherlands: history, character and new research. Geologie en Mijnbouw 79, 135–145.

Bungenstock, F., 2005. Der holozäne Meeresspiegelanstieg südlich der ostfriesischen Insel Langeoog, südliche Nordsee—hochfrequente Meeresspiegelbewegungen während der letzten 6000 Jahre. Ph.D. Thesis, University of Bonn, 184pp.

Caston, V.N.D., 1979. A new isopachyte map of the Quaternary of the North Sea. In: Oele, E., Schüttenhelm, R.T.E., Wiggers, A.J. (Eds), The Quaternary History of the North Sea. Acta Universitatis Upsaliensis, Symposia Universitatis Upsaliensis Annum Quingentesimum Celebrantis, vol. 2, Uppsala, pp. 23–28.

Cleveringa, P., Meijer, T., Van Leeuwen, R.J.W., de Wolf, H., Pouwer, R., Lissenberg, T., Burger, A.W., 2000. The Eemian stratotype locality at Amersfoort in the central Netherlands: a re-evaluation of old and new data. Geologie en Mijnbouw 79, 197–216.

Cohen, K.M., 2005. 3D geostatistical interpolation and geological interpolation of palaeo-groundwaterrise within the coastal prism in the Netherlands. In: Giosan, L., Bhattacharaya, J.P. (Eds.), River Deltas: Concepts, Models, and Examples. SEPM Special Publication, vol. 83. Tulsa, Oklahoma, pp. 341–364.

Denys, L., Baeteman, C., 1995. Holocene evolution of relative sea level and local mean high water spring tides in Belgium—a first assessment. Marine Geology 124, 1–19.

Dziewonski, A.M., Anderson, D.L., 1981. Preliminary reference Earth model. Physics of the Earth and Planetary Interiors 25, 297–356.

Fairbridge, R.W., 1961. Eustatic changes in sea level. Physics and Chemistry of the Earth 4, 100–185.

Farrell, W.E., Clark, J.A., 1976. On postglacial sea level. Geophysical Journal of the Royal Astronomical Society 46, 647–667.

Fjeldskaar, W., 1994. Viscosity and thickness of the asthenosphere detected from the Fennoscandian uplift. Earth and Planetary Science Letters 126, 399–410.

Fleming, K., Johnston, P., Zwartz, D., Yokoyama, Y., Lambeck, K., Chappell, J., 1998. Refining the eustatic sea-level curve since the Last Glacial Maximum using far- and intermediate-field sites. Earth and Planetary Science Letters 163, 327–342.

Franken, A., 1987. Rekonstruktie van het paleo-getijklimaat in de Noordzee. Rapport X0029-00, Waterloopkundig Lab, Delft, 74pp.

Gripp, K., 1964. Erdgeschichte in Schleswig-Holstein. Neumünster.

Gronwald, W., 1960. Welche Erkenntnisse zur Frage der vermuteten neuzeitlichen Nordseeküstensenkung hat die Wiederholung des deutschen Nordseeküstennivellements gebracht? Die Küste 8, 66–82.

Hinz, K., 1968. A contribution to the geology of the North Sea according to geophysical investigations by the geological survey of the German Federal Republic. In: Geology of Shelf Areas. Edinburgh, pp. 55–71.

Jelgersma, S., 1961. Holocene Sea Level Changes in the Netherlands. Van Aelst, Maastricht, 101pp.

Jelgersma, S., Oele, E., Wiggers, A.J., 1979. Depositional history and coastal development in The Netherlands and the adjacent North Sea since the Eemian. In: Oele, E., Schüttenhelm, R.T.E., Wiggers, A.J. (Eds.), The Quaternary History of the North Sea. Acta Universitatis Upsaliensis, Symposia Universitatis Upsaliensis Annum Quingentesimum Celebrantis, vol. 2, Uppsala, pp. 115–142.

Johnston, P., 1995. The role of hydro-isostasy for Holocene sea-level changes in the British Isles. Marine Geology 124, 61–70.

Kaufmann, G., Wu, P., 1998a. Upper mantle lateral viscosity variations and Post-Glacial rebound: application to the Barents Sea. In: Wu, P. (Ed.), Dynamics of the Ice Age Earth: a Modern Perspective. Trans Tech Publications, Zürich, Switzerland, pp. 583–602.

Kaufmann, G., Wu, P., 1998b. Lateral asthenospheric viscosity variations and postglacial rebound: a case study for the Barents Sea. Geophysical Research Letters 25 (11), 1963–1966.

Kaufmann, G., Wu, P., 2002. Glacial isostatic adjustment in Fennoscandia with a three-dimensional viscosity structure as an inverse problem. Earth and Planetary Science Letters 197 (1–2), 1–10.

Kaufmann, G., Wu, P., Li, G., 2000. Glacial isostatic adjustment in Fennoscandia for a laterally heterogeneous Earth. Geophysical Journal International 143 (1), 262–273.

Kaufmann, G., Wu, P., Ivins, E.R., 2005. Lateral viscosity variations beneath Antarctica and their implications on regional rebound motions and seismotectonics. Journal of Geodynamics 39 (2), 165–181.

Kiden, P., 1995. Holocene relative sea-level change and crustal movement in the southwestern Netherlands. Marine Geology 124, 21–41.

Kiden, P., Denys, L., Johnston, P., 2002. Late Quaternary sea-level change and isostatic and tectonic land movements along the Belgian–Dutch North Sea coast: geological data and model results. Journal of Quaternary Science 17, 535–546.

Kockel, F., 1995. Structural and palaeogeographical development of the German North Sea sector. Beitrage zur. Regionalen Geologie der Erde 26, 1–96.

Kooi, H., Johnston, P., Lambeck, K., Smither, C., Molendijk, R., 1998. Geological causes of recent (100 yr) vertical land movement in the Netherlands. Tectonophysics 299, 297–316.

Kudraß, H.-R., cruise participants, 2004. Cruise Report: North Sea BGR04-AUR/Leg 2. Internal Report, 93pp.

Lambeck, K., 1993a. Glacial rebound of the British Isles—I. Preliminary model results. Geophysical Journal International 115, 941–959.

Lambeck, K., 1993b. Glacial rebound of the British Isles—II. A high-resolution, high-precision model. Geophysical Journal International 115, 960–990.

Lambeck, K., 1995. Late Devensian and Holocene shorelines of the British Isles and North Sea from models of glacio-hydroisostatic rebound. Journal of Geological Society of London 152, 437–448.

Lambeck, K., 1997. Sea-level change along the French Atlantic and Channel coasts since the time of the Last Glacial Maximum. Paleogeography Paleoclimatology Paleoecology 129, 1–22.

Lambeck, K., 2002. In: Mitrovica, J.X., Vermeersen, L.L.A. (Eds.), Sea Level Change from Mid-Holocene to Recent Time: an Australian Example with Global Implications in Glacial Isostatic Adjustment and the Earth System: Sea Level, Crustal Deformation, Gravity and Rotation. AGU Monograph, Geodynamics Series, vol. 29, American Geophysical Union, Washington DC, pp. 33–50.

Lambeck, K., Bard, E., 2000. Sea-level change along the French-Mediterranean coast for the past 30,000 years. Earth and Planetary Science Letters 175, 203–222.

Lambeck, K., Johnston, P., Smither, C., Nakada, M., 1996. Glacial rebound of the British Isles: III. Constraints on mantle viscosity. Geophysical Journal International 125, 340–354.

Lambeck, K., Smither, C., Johnston, P., 1998a. Sea-level change, glacial rebound and mantle viscosity for northern Europe. Geophysical Journal International 134, 102–144.

Lambeck, K., Smither, C., Ekman, M., 1998b. Tests of glacial rebound models for Fennoscandia based on instrumented sea- and lake-level records. Geophysical Journal International 135, 375–387.

Lange, W., Menke, B., 1967. Beiträge zur frühpostglazialen erd- und vegetationsgeschichtlichen Entwicklung im Eidergebiet, insbesondere zur Flußgeschichte und zur Genese des sogenannten Basistorfes. Meyniana 17, 29–44.

Latychev, K., Mitrovica, J.X., Tamisiea, M.E., Tromp, J., Moucha, R., 2005a. Influence of lithospheric thickness variations on 3-D velocities due to glacial isostatic adjustment. Geophysical Research Letters 32.

Latychev, K., Mitrovica, J.X., Tromp, J., Tamisiea, M.E., Komatisch, D., Christara, C.C., 2005. Glacial isostatic adjustment on 3-D Earth models: a finite-volume formulation. Geophysical Journal International 161, 421–444.

Linke, G., 1982. Der Ablauf der holozänen Transgression der Nordsee aufgrund von Ergebnissen aus dem Gebiet Neuwerk/Scharhörn. Probleme der Küstenforschung im Südlichen Nordseegebiet 14, 123–157.

Louwe Kooijmans, L.P., 1974. The Rhine/Meuse Delta; four studies on its prehistoric occupation and Holocene geology. Ph.D. Thesis, University of Leiden, 421pp.

Ludwig, G., Müller, H., Streif, H., 1979. Neuere Daten zum holozänen Meeresspiegelanstieg im Bereich der Deutschen Bucht. Geologisches Jahrbuch D 32, 3–22.

Makaske, B., Van Smeerdijk, D.G., Peeters, H., Mulder, J.R., Spek, T., 2003. Relative water-level rise in the Flevo lagoon (The Netherlands), 5300–2300 cal. yr BC: an evaluation of new and existing basal peat time–depth data. Netherlands Journal of Geosciences 82, 115–131.

Milne, G.A., Long, A.J., Bassett, S.E., 2005. Modelling Holocene relative sea-level observations from the Caribbean and South America. Quaternary Science Reviews 24, 1183–1202.

Mörner, N.-A., 1980. The northwest European 'sea-level laboratory' and regional Holocene eustasy. Palaeogeography Palaeoclimatology Palaeoecology 29, 281–300.

Mostaert, F., De Moor, G., 1984. Eemian deposits in the neighbourhood of Brugge: a palaeogeographical and sea-level reconstruction. Bulletin de la Société belge de Géologie 93, 279–286.

Mostaert, F., De Moor, G., 1989. Eemian and Holocene sedimentary sequences on the Belgian coast and their meaning for sea level reconstruction. In: Henriet, J.P. De Moor, G. (Eds.), The Quaternary and Tertiary Geology of the Southern Bight, North Sea. Ministry of Economic Affairs, Belgian Geological Survey, Brussels, pp. 137–148.

Nakada, M., Lambeck, K., 1989. Late Pleistocene and Holocene sea-level change in the Australian region and mantle rheology. Geophysical Journal International 96, 497–517.

Paepe, R., Vanhoorne, R., Deraymaeker, D., 1972. Eemian deposits near Brugge (Belgian coastal plain). Belgische Geologische Dienst Professional Paper 1972/9, pp. 1–12.

Peltier, W.R., 2002. On eustatic sea level history: Last Glacial Maximum to Holocene. Quaternary Science Reviews 21, 377–396.

Pirazzoli, P.A., Pluet, J., 1991. World Atlas of Holocene Sea-Level Changes. Elsevier Oceanography Series, vol. 58, Elsevier, Amsterdam.

Reinhardt, L., cruise participants, 2006. Cruise Report: RV *Heincke* Cruise HE242 Leg 2—North Sea. Internal Report, 113pp.

Roeleveld, W., 1974. The Holocene evolution of the Groningen Marine-Clay District. Berichten van de Rijksdienst voor het Oudheidkundig Bodemonderzoek 24 (Suppl.).

Roeleveld, W., Gotjé, W., 1993. Holocene waterspiegelontwikkeling in de Noordoostpolder in relatie tot zeespiegelbeweging en kustontwikkeling. In: De Holocene laagveenontwikkeling in de randzone van de Nederlandse kustvlakte (Noordoostpolder). Ph.D. Thesis, Vrije Universiteit Amsterdam, pp. 76–86.

Roep, T.B., Beets, D.J., 1988. Sea-level rise and paleotidal levels from sedimentary structures in the coastal barrier in the western Netherlands since 5600 BP. Geologie en Mijnbouw 67, 53–60.

Schellmann, G., Radtke, U., 2004. The Marine Quaternary of Barbados. Kölner Geographische Arbeiten 81, 137.

Shennan, I., 1987. Holocene sea-level changes in the North Sea region. In: Tooley, M.J., Shennan, I. (Eds.), Sea-Level Changes. Basil Blackwell, Oxford, pp. 109–151.

Shennan, I., Horton, B., 2002. Holocene land- and sea-level changes in Great Britain. Journal of Quaternary Science 17 (5–6), 511–526.

Shennan, I., Lambeck, K., Horton, B., Innes, J., Lloyd, J., McArthur, J., Rutherford, M., 2000a. Holocene isostasy and relative sea-level changes on the east coast of England. In: Shennan, I., Andrews, J. (Eds.), Holocene Land—Ocean Interaction and Environmental Change Around the North Sea. Geological Society, London, Special Publications, vol. 166, pp. 275–298.

Shennan, I., Lambeck, K., Flather, R., Horton, B., McArthur, J., Innes, J., Lloyd, J., Rutherford, M., Wingfield, R., 2000b. Modelling western North Sea palaeogeographies and tidal ranges during the Holocene. In: Shennan, I., Andrews, J. (Eds.), Holocene Land–Ocean Interaction and Environmental Change Around the North Sea. Geological Society, London, Special Publications, vol. 166, pp. 299–319.

Spada, G., Antonioli, A., Cianetti, S., Giunchi, C., 2006. Glacial isostatic adjustment and relative sea-level changes: the role of lithospheric and upper-mantle heterogeneities in a 3-D spherical Earth. Geophysical Journal International 165, 692–792.

Steffen, H., Kaufmann, G., 2005. Glacial isostatic adjustment of Scandinavia and northwestern Europe and the radial viscosity structure of the Earth's mantle. Geophysical Journal International 163 (2), 801–812.

Steffen, H., Kaufmann, G., Wu, P., 2006. Three-dimensional finite-element modelling of the glacial isostatic adjustment in Fennoscandia. Earth and Planetary Science Letters 250, 358–375.

Streif, H., 2004. Sedimentary record of Pleistocene and Holocene marine inundations along the North Sea coast of Lower Saxony, Germany. Quaternary International 112, 3–28.

Streif, H., Uffenorde, H., Vinken, R., 1983. Untersuchungen zum pleistozänen und holozänen Transgressionsgeschehen im Bereich der südlichen Nordsee. Unpublished Internal Report, Niedersächsisches Landesamt für Bodenforschung, Hannover, 102pp.

Stuiver, M., Reimer, P., 1993. Extended ^{14}C database and revised CALIB radiocarbon calibration program. Radiocarbon 35, 15–230.

Stuiver, M., Reimer, P., Braziunas, T.F., 1998. High-precision radiocarbon age calibration for terrestrial and marine samples. Radiocarbon 40, 1127–1151.

Van de Plassche, O., 1982. Sea-level change and water-level movements in the Netherlands during the Holocene. Mededelingen Rijks Geologische Dienst 36 (1), 93.

Van de Plassche, O., 1986. Sea-Level Research: a Manual for the Collection and Evaluation of Data. Galliard (Printers) Ltd., Great Britain, 681pp.

Van de Plassche, O., 1995. Evolution of the intra-coastal tidal range in the Rhine–Meuse Delta and Flevo Lagoon, 5700–3000 yrs cal B.C. Marine Geology 124, 113–128.

Van de Plassche, O., Bohncke, S.J.P., Makaske, B., Van der Plicht, J., 2005. Water-level changes in the Flevo area, central Netherlands (5300–1500 BC): implications for relative mean sea-level rise in the Western Netherlands. Quaternary International 133–134, 77–93.

Van der Molen, J., de Swart, H.E., 2001. Holocene tidal conditions and tide-induced sand transport in the southern North Sea. Journal of Geophysical Research 106 (C5), 9339–9362.

Wessel, P., Smith, W.H.F., 1991. Free software helps map and display data. EOS 72, 441–446.

Wessel, P., Smith, W.H.F., 1998. New, improved version of generic mapping tools released. EOS 79, 579.

Wu, P., 2002. Mode coupling in a viscoelastic self-gravitating spherical earth induced by axisymmetric loads and lateral viscosity variations. Earth and Planetary Science Letters 202, 49–60.

Wu, P., 2005. Effects of lateral variations in lithospheric thickness and mantle viscosity on glacially induced surface motion in Laurentia. Earth and Planetary Science Letters 235, 549–563.

Wu, P., Van der Wal, W., 2003. Postglacial sealevels on a spherical, self-gravitating viscoelastic earth: effects of lateral viscosity variations in the upper mantle on the inference of viscosity contrasts in the lower mantle. Earth and Planetary Science Letters 211, 57–68.

Wu, P., Ni, Z., Kaufmann, G., 1998. Postglacial rebound with lateral heterogeneities: from 2D to 3D modeling. In: Wu, P. (Ed.), Dynamics of the Ice Age Earth: a Modern Perspective. Trans Tech Publication, Zürich Switzerland, pp. 557–582.

Wu, P., Wang, H.S., Schotman, H., 2005. Postglacial induced surface motions, sea levels and geoid rates on a spherical, self-gravitating laterally heterogeneous earth. Journal of Geodynamics 39 (2), 127–142.

Zagwijn, W.H., 1983. Sea-level changes in The Netherlands during the Eemian. Geologie en Mijnbouw 62, 437–450.

Zhong, S., Paulson, A., Wahr, J., 2003. Three-dimensional finite-element modelling of Earth's viscoelastic response: effects of lateral variations in lithospheric thickness. Geophysical Journal International 155, 679–695.

Zonneveld, I.S., 1960. De Brabantse Biesbosch. Ph.D. Thesis, University of Wageningen, 210pp.